Two receptor-like protein kinases, MUSTACHES and MUSTACHES-LIKE, regulate lateral root development in *Arabidopsis thaliana*

Qingqing Xun[1] (iD), Yunzhe Wu[1], Hui Li[1], Jinke Chang[1], Yang Ou[1], Kai He[1] (iD), Xiaoping Gou[1] (iD), Frans E. Tax[2] (iD) and Jia Li[1] (iD)

[1]Ministry of Education Key Laboratory of Cell Activities and Stress Adaptations, School of Life Sciences, Lanzhou University, Lanzhou 730000, China; [2]Department of Molecular and Cellular Biology, University of Arizona, Tucson, AZ 85721, USA

Author for correspondence:
Jia Li
Tel: +86 0931 8915662
Email: lijia@lzu.edu.cn

Summary

- Receptor-like protein kinases (RLKs) play key roles in regulating plant growth, development and stress adaptations. There are at least 610 RLKs (including receptor-like cytoplasmic kinases) in Arabidopsis. The functions of the majority of RLKs have not yet been determined.
- We previously generated promoter::*GUS* transgenic plants for all leucine-rich repeat (*LRR*)-*RLKs* in Arabidopsis and analyzed their expression patterns during various developmental stages. We found the expression of two *LRR-RLKs*, *MUSTACHES* (*MUS*) and *MUSTACHES-LIKE* (*MUL*), are overlapped in lateral root primordia. Independent mutants, *mus-3 mul-1* and *mus-4 mul-2*, show a significantly decreased emerged lateral root phenotype.
- Our analyses indicate that the defects of the double mutant occur mainly at stage I of lateral root development. Exogenous application of auxin can dramatically enhance the transcription of *MUS*, which is largely dependent on AUXIN RESPONSE FACTOR 7 (ARF7) and ARF19. MUS and MUL are inactive kinases *in vitro* but are phosphorylated *in planta*, possibly by an unknown kinase. The kinase activity of MUS is dispensable for its function in lateral root development. Many cell wall related genes are down regulated in *mus-3 mul-1*.
- In conclusion, we identified MUS and MUL, two kinase-inactive RLKs, in controlling the early development of lateral root primordia likely via regulating cell wall synthesis and remodeling.

Introduction

Plant growth, development, and adaptation to various stresses largely rely on cell-to-cell and cell-to-environment communications. Roots are important organs anchoring plants in soil and directly sensing signals from their surrounding environments. Roots also absorb water and nutrients from soil to provide fundamental compounds to plants for survival (Bellini *et al.*, 2014). Dicotyledonous plants mainly possess a taproot system, consisting of a primary root and numerous lateral roots. Lateral roots, including their number, length and distribution, play a key role in determining the entire architecture of a root system, directly associating with its biological functions (Lynch, 1995). Initiation and development of lateral root are regulated by both internal and external signals (Malamy, 2005). Molecular mechanisms controlling lateral root development, however, are poorly understood.

In model plant Arabidopsis, transverse section of a primary root exhibits a pattern organized in concentric layers, consisting of epidermis, cortex, endodermis, pericycle, and vascular tissues from outside to inside (Dolan *et al.*, 1993; Verbelen *et al.*, 2006).

The pericycle contains two different types of cells, phloem-pole-pericycle cells and xylem-pole-pericycle (XPP) cells (Mähönen *et al.*, 2006; Parizot *et al.*, 2008). Differentiated XPP cells have the ability to re-initiate cell division, the first step of lateral root development, and these XPP cells are named lateral root founder cells (Casimiro *et al.*, 2003). Lateral root organogenesis can be divided into four steps, lateral root positioning, lateral root initiation, lateral root primordium development and lateral root primordium emergence (Du & Scheres, 2018). Lateral root positioning determines the spatial arrangement of lateral roots along a primary root (Van Norman *et al.*, 2013). Lateral roots initiate from regularly spaced lateral root founder cells, undergoing the first asymmetric cell division (Dubrovsky *et al.*, 2000). Lateral root primordium development can be artificially classified into eight different stages, stages I–VIII. A new meristem is gradually established through lateral root primordium cell division, differentiation and growth (Malamy & Benfey, 1997; Benková & Bielach, 2010). As the lateral root primordia develops, it emerges from the primary root by crossing the overlying endodermis, cortex and epidermis (Kumpf *et al.*, 2013; Vilches-Barro & Maizel, 2015).

Cell-to-cell and cell-to-environment communications are critical during lateral root development. Receptor-like protein kinases (RLKs) are a group of transmembrane proteins playing significant roles in these communications (Walker & Zhang, 1990). RLKs contain an extracellular domain mainly involved in perceiving small molecules from adjacent cells or from the surrounding environment, a single-pass transmembrane domain anchoring the protein to the plasma membrane, and a cytoplasmic kinase domain responsible for transducing an extracellular signal to a cellular signaling cascade predominantly via protein phosphorylation and dephosphorylation (Shiu & Bleecker, 2001). There are at least 610 RLKs and receptor-like cytoplasmic kinases (RLCKs) in the model plant Arabidopsis (Shiu & Bleecker, 2001). Based on the composition of the extracellular domain, Arabidopsis RLKs can be grouped into more than 21 subfamilies, in which leucine-rich repeat (LRR)-RLKs belong to the most abundant subfamily. There are at least 223 LRR-RLKs in Arabidopsis (Shiu & Bleecker, 2001; Gou *et al.*, 2010; Wu *et al.*, 2016). Generally, RLKs play fundamental roles in regulating both plant development and defense (Li & Tax, 2013). Functional characterization of receptor kinases has become one of the frontiers in plant biology. Up to date, only a small fraction of RLKs has been functionally defined, and the majority of them still need to be functionally characterized.

It has been reported that several RLKs regulate lateral root growth, development, and adaptations to various adverse environments. For example, Arabidopsis CRINKLY4 (ACR4) is involved in controlling the division of lateral root founder cells during lateral root initiation and lateral root primordium development at stage I (Gifford *et al.*, 2005; De Smet *et al.*, 2008). HAESA (HAE), HAESA-LIKE 2 (HSL2), and their peptide ligand INFLORESCENCE DEFICIENT IN ABSCISSION (IDA) play important functions in controlling cell separation during lateral root emergence (Kumpf *et al.*, 2013). Under heterogeneous nitrogen conditions, CEP RECEPTOR 1 (CEPR1) and CEPR2 can perceive C-TERMINALLY ENCODED PEPTIDE 1 (CEP1), which can be transported through roots and shoots, and ultimately promote the growth of lateral roots where there are sufficient nitrogen sources, and dampen the growth under nutrient-poor conditions (Tabata *et al.*, 2014; Ohkubo *et al.*, 2017). This strategy helps plants to coordinate regulation and adapt to the heterogeneity of the soil environment by controlling lateral root growth (Bisseling & Scheres, 2014; Dimitrov & Tax, 2018). When nitrogen is deficient, CLAVATA 3/EMBRYO SURROUNDING REGION (CLE) 1, CLE3, CLE4 and CLE7 can be synthesized and secreted in the pericycle layer, which are perceived by CLAVATA 1 (CLV1) in the adjacent phloem cells, inhibiting lateral root formation (Araya *et al.*, 2014). ROOT MERISTEM GROWTH FACTOR 1 (RGF1) can reduce the lateral root numbers of Columbia-0 (Col-0). Lateral roots of a quadruple mutant *rgi1,2,3,4* of the RGF1 receptors, RGF1 INSENSITIVES (RGIs), cannot be inhibited by RGF1 (Ou *et al.*, 2016). In addition, TRACHEARY ELEMENT DIFFEENTIATION INHIBITORY FACTOR (TDIF) and its receptor PHLOEM INTERCALATED WITH XYLEM (PXY) interact with

BRASSINOSTEROID-INSENSITIVE2 (BIN2) in pericycle and regulate lateral root development by promoting auxin signal transduction (Okushima *et al.*, 2007; Cho *et al.*, 2014). Loss of function mutants in the PEPTIDE RAPID ALKALINIZATION FACTOR (RALF) 34 and its receptor THESEUS1 (THE1) show irregular asymmetric founder cell divisions during lateral root initiation (Murphy *et al.*, 2016; Gonneau *et al.*, 2018). In a recent study, it was found that peptide hormone TARGET OF LBD SIXTEEN2 (TOLS2) and its receptor RECEPTOR-LIKE KINASE7 (RLK7) govern the number of lateral root founder cells, negatively regulating lateral root initiation and ensuring proper lateral root spacing (Toyokura *et al.*, 2019).

Our laboratory is mainly interested in revealing the biological function of RLKs, especially LRR-RLKs, in model plant Arabidopsis. From a previous study (Wu *et al.*, 2016), we identified a receptor kinase, encoded by *At1G75640*, that is mainly expressed during lateral root initiation and development. This gene was previously named *MUSTACHES* (*MUS*) (Keerthisinghe *et al.*, 2015). MUS protein was identified in stomata and regulates stomatal bilateral symmetry, although we failed to detect its expression in *pMUS::GUS* transgenic plants possibly due to the limitation of the GUS staining approach we used. Here we report a new role of MUS in regulating lateral root development. Our phylogenetic analysis indicated that MUS has a closely related protein which is encoded by *At4G36180* and we subsequently named it as MUSTACHES-LIKE (MUL). *In vitro* analysis indicated MUS and MUL are kinase-inactive RLKs. However, MUS and MUL can be phosphorylated *in planta*, possibly by another undetermined kinase. Single loss-of-function mutants of *MUS* and *MUL*, including *mus-3*, *mus-4*, *mul-1* and *mul-2*, show no lateral root developmental defects. However, two independent double mutants, *mus-3 mul-1* and *mus-4 mul-2*, show significantly decreased emerged lateral root density. Further investigation using one of the two independent double mutants, *mus-3 mul-1*, revealed that the decreased emerged lateral root phenotype of the double mutant is not caused by defects in the initiation of lateral root primordia, but mainly by delayed lateral root primordium development at stage I. Interestingly, MUS was found to have a polar localization in primary and lateral root cells. Exogenous application of auxin can dramatically enhance the expression of *MUS* in the primary root differentiation zone and in the lateral root primordia. The upregulation of *MUS* by auxin is AUXIN RESPONSE FACTOR 7 (ARF7) and ARF19 dependent. RNA-seq data showed that MUS and MUL affect lateral root development likely via regulating cell wall biosynthesis and remodeling. In summary, we found MUS and MUL are kinase-inactive RLKs and play an important role during an early stage of lateral root development.

Materials and Methods

Plant materials and growth conditions

Wild-type and mutants used in this study are all in *Arabidopsis thaliana* ecotype Col-0 background. The T-DNA insertion lines were obtained from the Arabidopsis Biological Resource Center

(ABRC), including *mus-3* (SALK_101029), *mus-4* (SALK_072166), *mul-1* (SALK_042322), *mul-2* (GK-593C11), *arf7-1 arf19-1* (CS24629). All plants were grown in glasshouses (16 h light and 8 h dark, 22°C). For seedling experiments, seeds were sterilized in 75% ethanol for 1 min and 1% sodium hypochlorite for 10 min, and washed in double distilled water (ddH$_2$O) five times. The seeds were then vernalized at 4°C for 2 d. Seeds were germinated and the seedlings were grown on ½ Murashige and Skoog (MS) plates containing 1% sucrose and 0.9% agar in a growth chamber with 16 h light and 8 h dark at 22°C. For liquid culture, seeds in ½MS liquid medium were shaken gently at 120 rpm under the same growing condition.

Generation of double mutants and transgenic plants

Double mutants *mus-3 mul-1* and *mus-4 mul-2* were obtained by crossing single mutants *mus-3, mul-1, mus-4, mul-2*, correspondingly. The promoter and coding sequences of *MUS*, *MUL* and *BAM2* were amplified with primers listed in the Supporting Information Table S1. The PCR products were cloned into an entry vector *pDONR/Zeo* using a BP reaction (Invitrogen, Carlsbad, CA, USA). The sequences from the obtained entry clones were recloned into an appropriate destination vector. For expression pattern analyses, the promoter sequences of *MUS* (2160 bases before translation initiation codon) and *MUL* (1276 bases before translation initiation codon) were cloned into the *pBIB-BASTA-GUS-GWR* vector. For protein localization and complementation, genomic sequences driven by the native promoter of *MUS* or *MUL* were cloned into *pBIB-BASTA-GWR-YFP* and *pBIB-BASTA-GWR-GFP*, respectively. For phosphorylation analyses *in planta*, the coding sequences of *MUS*, *MUL* and *BAM2* were cloned into *pBIB-BASTA-UBQ10-GWR-FLAG*. The arginine (R) at 867 aa of MUS or at 869 aa of MUL, the ATP binding sites, were mutated to a glutamic acid (E) and lysine (K) by PCR-mediated mutagenesis. The mutated gene was also cloned into *pBIB-BASTA-UBQ10-GWR-FLAG*. All transgenic plants were generated by the floral dip method using *Agrobacterium tumefaciens* GV3101 strain. All the vectors were used to construct transgenic plants in this article as described previously (Gou *et al.*, 2010).

Staining and microscopic analyses

Homozygous seedling lines of *pMUS::GUS* and *pMUL::GUS* were incubated in a GUS staining solution at 37°C for 6 h as described previously (Wu *et al.*, 2016), and then were decolorized by a gradient of ethanol solutions. Whole plants were analyzed and photographed using a stereomicroscope (M165C; Leica, Weztlar, Germany). The primary roots and the lateral root primordia were cleared with two clearing solutions, solution made by mixing chloral hydrate, glycerol, water (4 : 1 : 1, w/w/w) for Fig. 1, and another clearing solution as reported previously (Malamy & Benfey, 1997). A microscope (DM6000B; Leica) was used for analyzing and photographing the root GUS staining. For protein localization of MUS, MUL, PIN1 and PIN3, the corresponding seedlings were stained in 100 ng µl^{-1} propidium

iodide (PI) for 8 min. For stomatal phenotypes of Col-0, *mus-3*, *mul-1* and *mus-3 mul-1*, the corresponding seedlings were stained in 25 ng µl^{-1} SynaptoRed C2 (FM4-64) (70021; Biotium, Fremont, CA, USA) for 30 min. Seedlings were photographed using a confocal fluorescence microscope (TCS SP8; Leica).

RNA extraction and transcription analysis

Total RNA from Col-0 and *mus-3 mul-1* plants was extracted from 7-d-old seedling roots by using an RNeasy Plant Mini Kit (74903; Qiagen, Hilden, Germany) for RNA-seq or total RNA pure Plant Kits (DP437; Tiangen; Beijing, China) for quantitative reverse transcription polymerase chain reaction (qRT-PCR). The purified RNA was used for synthesizing the cDNA by using M-MLV reverse transcriptase (C28025; Invitrogen, Carlsbad, CA, USA). The cDNA was used to test homozygous T-DNA insertions of genes by RT-PCR. Relative expression levels were obtained after normalized by *ACTIN2*. The primers used for RT-PCR and qRT-PCR are shown in Table S1.

Lateral root induction

Seedlings were grown on ½MS for 3 d after germination. The primary root tip was artificially bent to 90° with the root tip pointing towards the gravity. The roots were collected every 6 h and stained with GUS solution before analyzing under a microscope (DM6000B; Leica).

IAA treatment

The *pMUS::GUS* and *pMUL::GUS* transgenic plants were grown on ½MS medium for 8 d, then treated with 0.01% dimethyl sulfoxide (DMSO) or 1 µM indole-3-acetic acid (IAA) liquid medium for 12 h, stained with GUS solution for 2 h and photographed with a Leica microscope, as described earlier. Col-0, *arf7-1 arf19-1* seedlings were grown on 1/5 MS medium for 8 d, and treated in 1 µM IAA liquid medium for 3 h. Total RNA was extracted from the seedling roots and expression levels of *MUS* and *MUL* were detected by qRT-PCR.

Protein induction, purification, phosphorylation assays *in vitro*

For *in vitro* induction and purification of proteins, the cDNA sequence coding of cytoplasmic domains (CDs) of MUS and the kinase domain (KD) of CLV1 were cloned into a *pDEST15* vector with an in-frame GST tag. Whereas the cDNA sequence coding for the cytoplasmic domain of MUL was cloned into *pET-15b* with an in-frame His tag. The resulting construct was transformed into *Escherichia coli* Rosetta for protein expression with isopropyl-β-D-thiogalactoside (IPTG) induction. GST-MUS$_{CD}$, GST-MUS$_{CD}$^{R867E}, GST-MUS$_{CD}$^{R867K}, His-MUL$_{CD}$, His-MUL$_{CD}$^{R869E}, His-MUL$_{CD}$^{R869K}, GST and GST-CLV1$_{KD}$ were purified by using glutathione agarose beads (C600031; Sangon Biotech, Shanghai, China) in binding buffer (50 mM Tris-HCl (pH 7.9), 100 mM sodium chloride (NaCl), 0.2% NP40, 10%
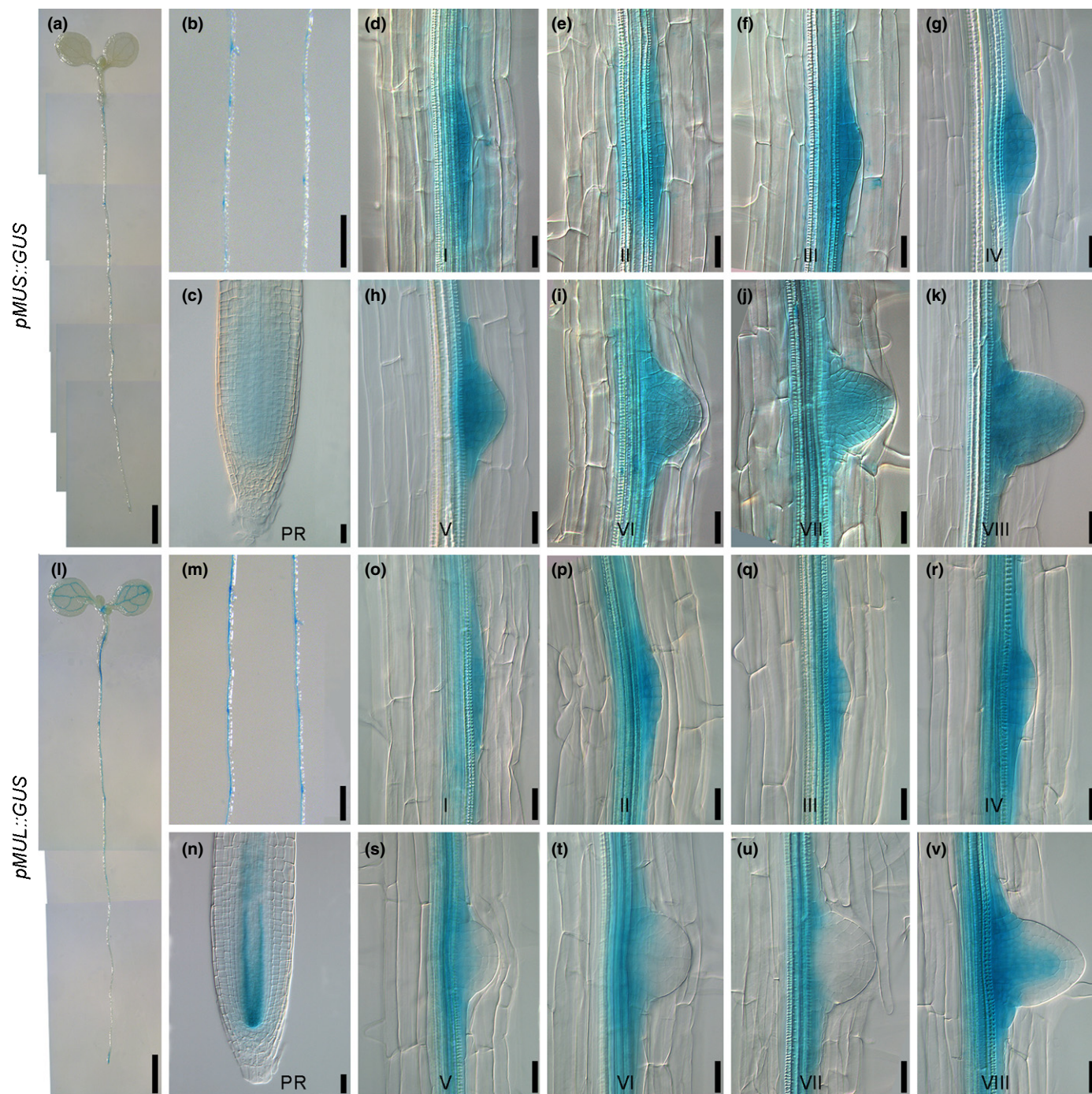
Fig. 1 The expression patterns of *MUS* and *MUL* in roots. (a–c) *MUS* is mainly expressed in lateral roots and weakly expressed in the meristematic zone of the primary roots. (d–k) *MUS* is expressed in the lateral root primordia at all eight different developmental stages. (l–v) *MUL* is expressed in the vasculature of the seedlings and in the early stages of lateral root formation. The seedlings used for GUS staining were 5 d (a–c, l–n) or 8 d (d–k, o–v) after germination. PR represents primary root. I–VIII represent the eight development stages of lateral root primordia. Bars: (a, l) 2mm; (b, m) 1mm; (c–k, n–v) 25 μm.

glycerol, 1 mM dithiothreitol (DTT), 0.5 mM phenylmethylsulfonyl fluoride (PMSF)) at 4°C for 3 h.

Phosphorylation was assayed as described previously with modifications (Li *et al.*, 2002). For *in vitro* phosphorylation assays, 1 μg of purified GST-CLV1$_{KD}$, GST-MUS$_{CD}$, GST-MUS$_{CD}$^{R867E}, GST-MUS$_{CD}$^{R867K}, His-MUL$_{CD}$, His-MUL$_{CD}$^{R869E}, His-MUL$_{CD}$^{R869K}, GST, MBP substrate were incubated with gentle shaking in the kinase assay buffer 20 mM Tris-HCl (pH 7.6), 1 mM DTT, 10 mM magnesium chloride (MgCl$_2$), 1 mM manganese chloride (MnCl$_2$), 0.1 mM ATP) containing 1 μl [γ-^{32}P]ATP at 30°C for 1 h. The proteins were mixed with 2 × SDS loading buffer and boiled for 5 min. The

proteins were separated by 12% SDS-PAGE (sodium dodecyl sulfate–polyacrylamide gel electrophoresis), quantitated by Coomassie brilliant blue and analyzed by autoradiography.

Total protein extraction and *in planta* phosphorylation assays

Ten-day-old transgenic seedlings from liquid culture were ground to powder and lysed in extraction buffer (10 mM HEPES (pH 7.5), 100 mM NaCl, 1 mM ethylenediaminete-traacetic acid (EDTA), 10% glycerol, 0.5% Triton X-100, complete protease inhibitor cocktail (04693132001; Roche, Basel, Swizerland) and phosphatase inhibitors). The super-natant was incubated with anti-FLAG beads (A2220; Sigma, St Louis, MO, USA) and gently shaken at 4°C for 3 h. The beads were washed three times with the extraction buffer. Proteins bound to the beads were mixed with 1 × SDS load-ing buffer and boiled for 5 min. The proteins were then ana-lyzed by immunoblotting with anti-FLAG antibody (M20008L; Abmart, Shanghai, China) for quantification or with anti-pThr antibody (9381S; Cell Signaling Technology, Boston, MA, USA) for phosphorylation analysis.

Results

MUS is mainly expressed in lateral root primordia

Within the last two decades, our laboratory has been mainly focusing on elucidating the biological functions of RLKs in Arabidopsis. We generated promoter::GUS transgenic plants for all 223 LRR-RLKs and analyzed their detailed expression patterns (Wu *et al.*, 2016). A number of tissue-specifically expressed RLKs were identified during these assays. One of these RLKs, At1G75640, is predominantly expressed during lateral root development. This gene, previously reported as MUSTACHES (MUS), was found to be involved in stomatal development (Keerthisinghe *et al.*, 2015). Our GUS staining analysis indicated that MUS is strongly expressed in the spots where lateral roots are formed and weakly expressed in the meristematic zone of primary roots (Fig. 1a–c). The expression of MUS, based on our GUS analysis, is beyond the detection levels in rosette leaves, inflorescences, flowers and siliques (Supporting Information Fig. S2a–d, see later). Detailed inves-tigations were carried out in cleared seedlings by using chloral hydrate solution (chloral hydrate, glycerol, water (4 : 1 : 1, w/ w/w)), revealing that MUS is expressed during all eight devel-opment stages of lateral root primordia (Fig. 1d–k).

The unique expression patterns of MUS suggest that MUS may be involved in lateral root development. We therefore set to examine the biological function of MUS in lateral root develop-ment. MUS is a member of the LRR-RLK subfamily VII. This subfamily contains 10 members. Phylogenetic analysis based on full-length amino acid sequences of subfamily VII members indi-cated that the closest paralog of MUS is At4G36180, which was subsequently named as MUSTACHES-LIKE (MUL) (Fig. S1). Analysis of transgenic plants harboring pMUL::GUS showed that

MUL is expressed not only in lateral roots but also in other tissues (Fig. 1l). Detailed analysis indicated that MUL is also expressed in young leaves, shoot apical meristems of 2-wk-old seedlings, pistils, the transmitting tract of pollen tubes, at the junction of siliques and petioles, in lateral root primordia stages I–IV, and also in the vascular tissue at stage VIII (Figs 1l–v, S2e–h). The overlapping expression patterns of MUS and MUL in lateral root development suggest MUS and MUL may play redundant roles during early stages of lateral root development.

Both *mus-3 mul-1* and *mus-4 mul-2* double mutants show a significantly reduced lateral root formation phenotype

To test whether MUS and MUL are truly involved in lateral root development, we obtained two independent T-DNA insertion lines for both MUS and MUL, named mus-3, mus-4, mul-1 and mul-2, respectively (Fig. 2a). RT-PCR analysis with primers that amplify full-length transcripts of MUS and MUL confirmed that the two independent T-DNA insertion lines for both genes are true null alleles (Fig. 2b). All of the single knockout mutants showed primary and lateral roots indistinguishable from those of wild type (Fig. S3a–d). These results suggest that MUS and MUL may play functionally redundant roles. To test this hypoth-esis, two independent double mutants, mus-3 mul-1 and mus-4 mul-2 were generated by genetic crosses. Interestingly, both mus-3 mul-1 and mus-4 mul-2 seedlings displayed slightly shortened primary roots and significantly less emerged lateral roots com-pared to wild-type Col-0 (Fig. 2c–f). The emerged lateral root densities (number of lateral roots/root length) of mus-3 mul-1 and mus-4 mul-2 were nearly half of those from Col-0 (Fig. 2f). The aerial parts of the mutants showed no obvious differences from Col-0 (Fig. S3e). Because mus-3 mul-1 and mus-4 mul-2 showed identical root defects, further analyses were mainly focused on mus-3 mul-1.

In order to further confirm the decreased lateral root density phenotype of mus-3 mul-1 was indeed due to the absence of both MUS and MUL, we constructed binary constructs pMUS::MUS-YFP and pMUL::MUL-YFP, and transferred them into mus-3 mul-1 respectively. More than 10 independent transgenic lines for each construct were subsequently generated. Transgenic plants with only one T-DNA insertion event, which was deter-mined via segregation analysis in T$_2$, were selected and homozy-gous lines were subsequently obtained. Seeds of two randomly selected independent homozygous transgenic lines from each construct were planted on ½MS medium, with Col-0 and mus-3 mul-1 as controls. The results indicated that two independent lines of pMUS::MUS-YFP in mus-3 mul-1 or pMUL::MUL-YFP in mus-3 mul-1 showed completely complemented primary and lateral root phenotypes, similar to wild type Col-0 (Fig. 3a–c). Consistently, qRT-PCR analysis indicated that, in all indepen-dent transgenic lines of pMUS::MUS-YFP in mus-3 mul-1 or pMUL::MUL-YFP in mus-3 mul-1, the expression of MUS or MUL was recovered to the level either similar or higher than Col-0 (Fig. 3d,e). These results demonstrate that the lateral root defective phenotype of mus-3 mul-1 is indeed caused by the simultaneous knockouts of both MUS and MUL.
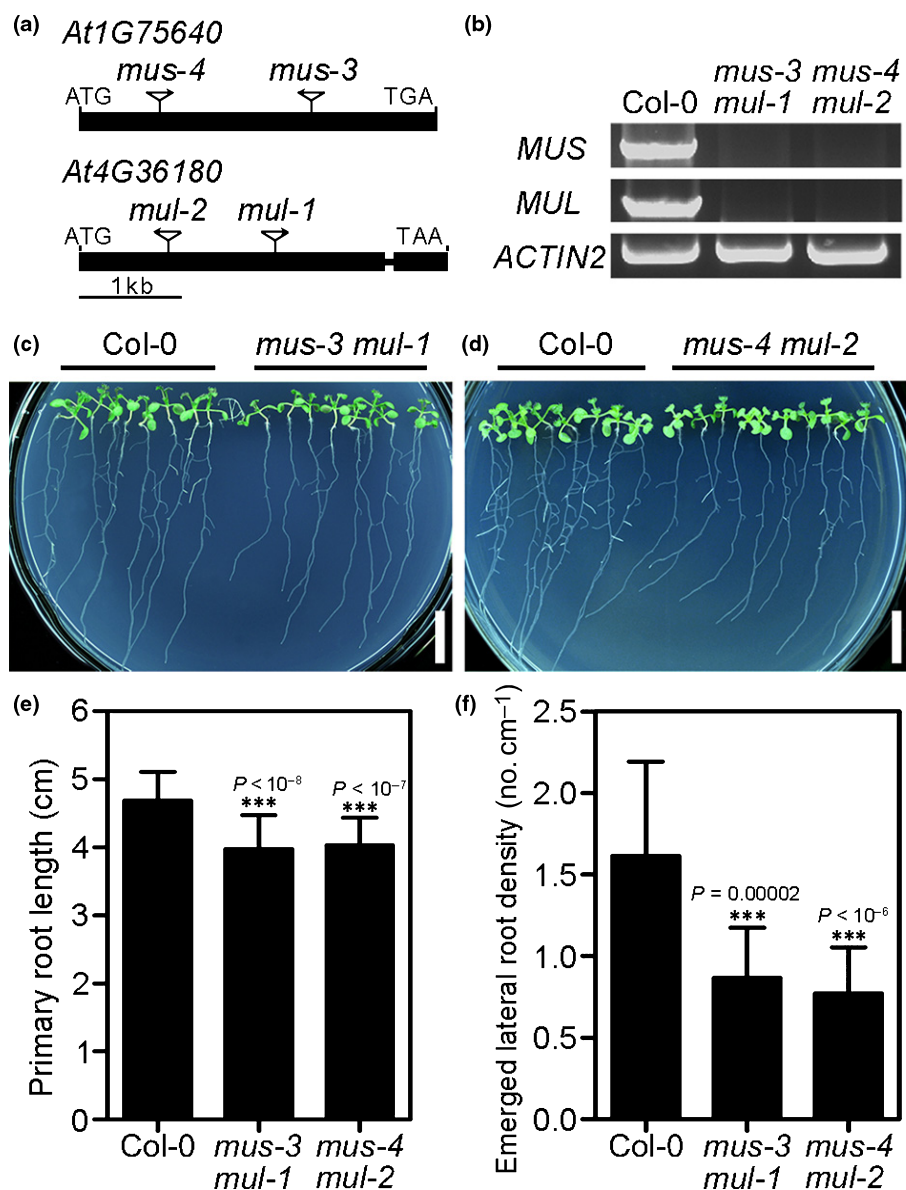
Fig. 2 Two independent double mutants, *mus-3 mul-1* and *mus-4 mul-2*, show a similar lateral root defective phenotype. (a) Diagrams showing the T-DNA insertion sites of two independent alleles for *MUS* (*mus-3* and *mus-4*) and *MUL* (*mul-1* and *mul-2*). The insertion sites of the T-DNA are indicated as triangles and the T-DNA orientations are marked with arrows. (b) RT-PCR results show no full length transcripts for both *MUS* and *MUL* in two independent double mutants. (c, d) Both *mus-3 mul-1* and *mus-4 mul-2* show significantly reduced number of emerged lateral roots than Col-0. The seedlings used for the photograph were 9 d after germination. Bars, 1 cm. (e, f) Measurements of primary root length and emerged lateral root density of Col-0, *mus-3 mul-1* and *mus-4 mul-2*. Data shown represent average and SD ($n > 30$). Student's *t*-tests were used to compare the measurements from *mus-3 mul-1* and *mus-4 mul-2* with those from Col-0 (***, $P < 0.001$).

MUS and MUL regulate lateral root primordia at an early developmental stage

To understand the detailed mechanisms of MUS and MUL in regulating lateral root development, we investigated the specific stages in which Col-0 and *mus-3 mul-1* show developmental differences. Decreased emerged lateral roots may be caused by defects at the initiation stage of lateral roots, lateral root primordium emergence, or developmental abnormalities in lateral root primordia. At early developmental stages, lateral root primordia are tiny and easily miscounted under a microscope. Auxin is known to accumulate at all developmental stages of lateral root primordia. To facilitate our analysis, we transformed *pDR5::GUS* into Col-0 and *mus-3 mul-1*, and counted the primordia in both *pDR5::GUS* in Col-0 and *pDR5::GUS* in *mus-3 mul-1* transgenic seedlings after GUS staining. Our data suggested that the density of stage I lateral root primordia in *mus-3 mul-1* was significantly

greater than that of Col-0, nearly twice that of Col-0 (Fig. 4a). The density of stages II–VIII lateral root primordia in Col-0 and *mus-3 mul-1* showed no significant differences. The density of nonemerged lateral roots in *mus-3 mul-1* was dramatically increased compared to that of wild type. The density of emerged lateral roots in *mus-3 mul-1*, however, was significantly decreased relative to Col-0, although the densities of total lateral roots (emerged and nonemerged together) in *mus-3 mul-1* and Col-0 showed no significant difference (Fig. 4a). These results indicated that MUS and MUL play an important role mainly at stage I of lateral root primordium development.

To further confirm the prominent role of MUS and MUL in lateral root primordium development, we designed a lateral root induction experiment based on an early observation that bending roots can induce lateral root formation at the convex surface due to the preferential accumulation of auxin (Ditengou *et al.*, 2008; Moreno-Risueno *et al.*, 2010). Seedlings were grown on ½MS
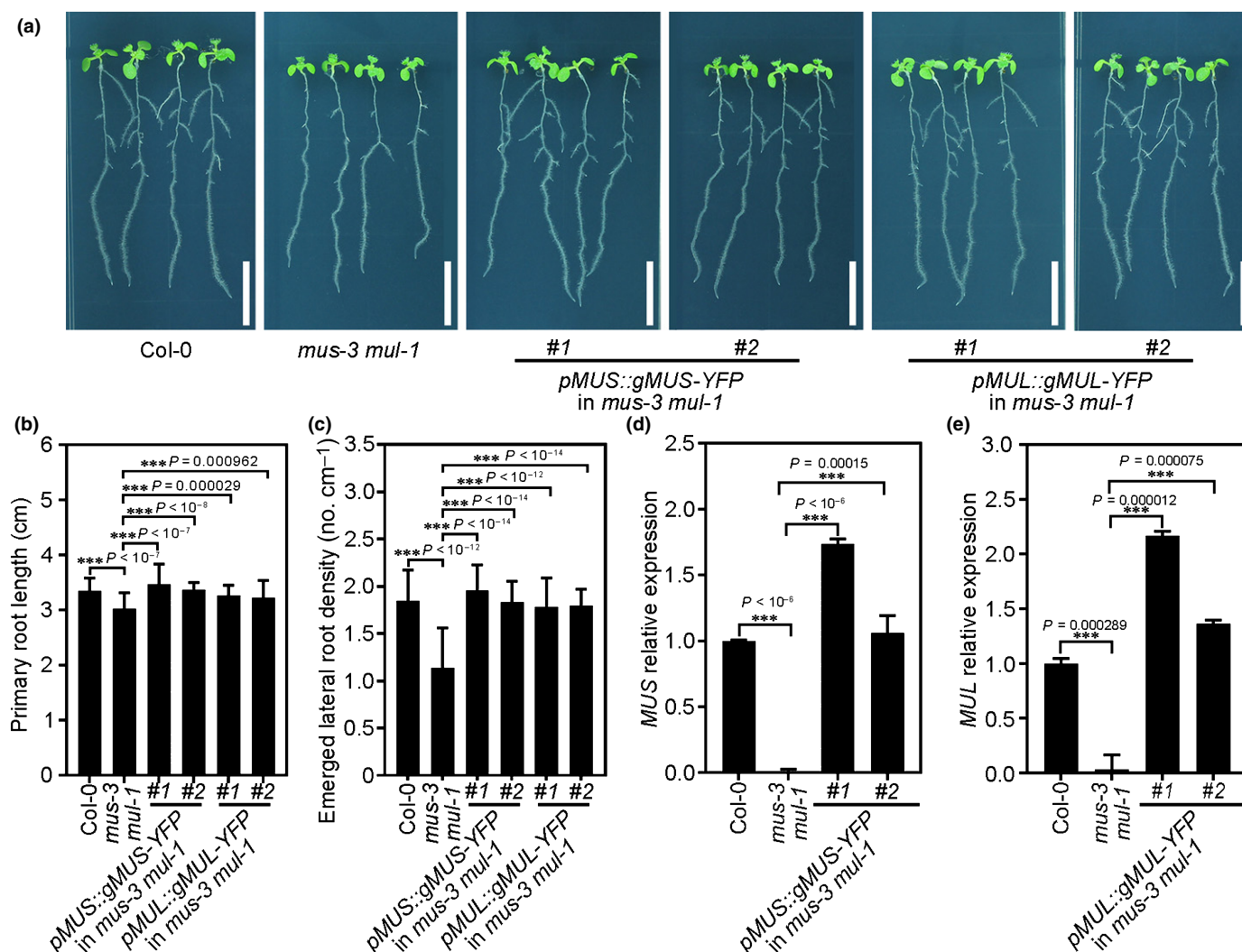
Fig. 3 Expression of *MUS* or *MUL* driven by their respective native promoters can rescue the lateral root defects of *mus-3 mul-1*. (a) Root phenotypes of Col-0, *mus-3 mul-1*, and two independent transgenic lines of *pMUS::gMUS-YFP* and *pMUL::gMUL-YFP* in *mus-3 mul-1*. The seedlings used for photographs and measurements were 9 d after germination. Bars, 1 cm. (b, c) Measurements of primary root length and emerged lateral root density of the seedlings, respectively. Data shown represent average and SD ($n > 25$). (d, e) qRT-PCR results indicating the relative expression levels of *MUS* and *MUL* in Col-0, *mus-3 mul-1*, *pMUS::gMUS-YFP* in *mus-3 mul-1*, and *pMUL::gMUL-YFP* in *mus-3 mul-1*. Data shown represent average and SD ($n = 3$). Student's *t*-test was used to compare the measurements from wild-type Col-0, two independent transgenic lines of *pMUS::gMUS-YFP* in *mus-3 mul-1*, and *pMUL::gMUL-YFP* in *mus-3 mul-1* with those from *mus-3 mul-1* (***, $P < 0.001$).

medium for 3 d after germination, and then placed horizontally with their primary root tips bending 90° towards the gravity (Fig. 4b). After different induction times, the roots were collected for further analyses. After 6 and 12 h of lateral root induction, the percentage of stage I lateral root primordia were almost the same between Col-0 and *mus-3 mul-1* at the bending site, indicating that the initiation of lateral root primordia is unaffected in *mus-3 mul-1* (Fig. 4c). Interestingly, after 30 h, Col-0 lateral root primordia were all developed at stage II and beyond, while 41% lateral root primordia in *mus-3 mul-1* were still at stage I (Fig. 4c). After 48 h, 8.4% lateral root primordia in *mus-3 mul-1* were still at stage I, whereas all the lateral root primordia in wild type were already developed at stage III and beyond (Fig. 4c). These results further confirmed that MUS and MUL regulate the development of the lateral root primordia at stage I.

The completion of lateral root initiation represents the beginning the stage I of lateral root primordium development, which contains four cells, two big and two small ones (Malamy & Benfey, 1997). After several anticlinal divisions, there are six or more cells at stage I. The center cells of stage I undergo a periclinal division and produce two layers of cells, symbolizing the beginning of stage II (Malamy & Benfey, 1997). In order to uncover what causes lateral roots to be retained at stage I in *mus-3 mul-1*, we counted cell numbers in Col-0 and *mus-3 mul-1* at stage I just after the first periclinal division starts. Statistical analysis showed that in Col-0 the first periclinal division occurs when 5.7 cells are formed at stage I (Fig. 4d). However, in *mus-3 mul-1* the first periclinal division occurs when 6.7 cells are formed at stage I (Fig. 4d). It was reported that cell width of the center founder cells affects early development of lateral root (Vermeer *et al.*,
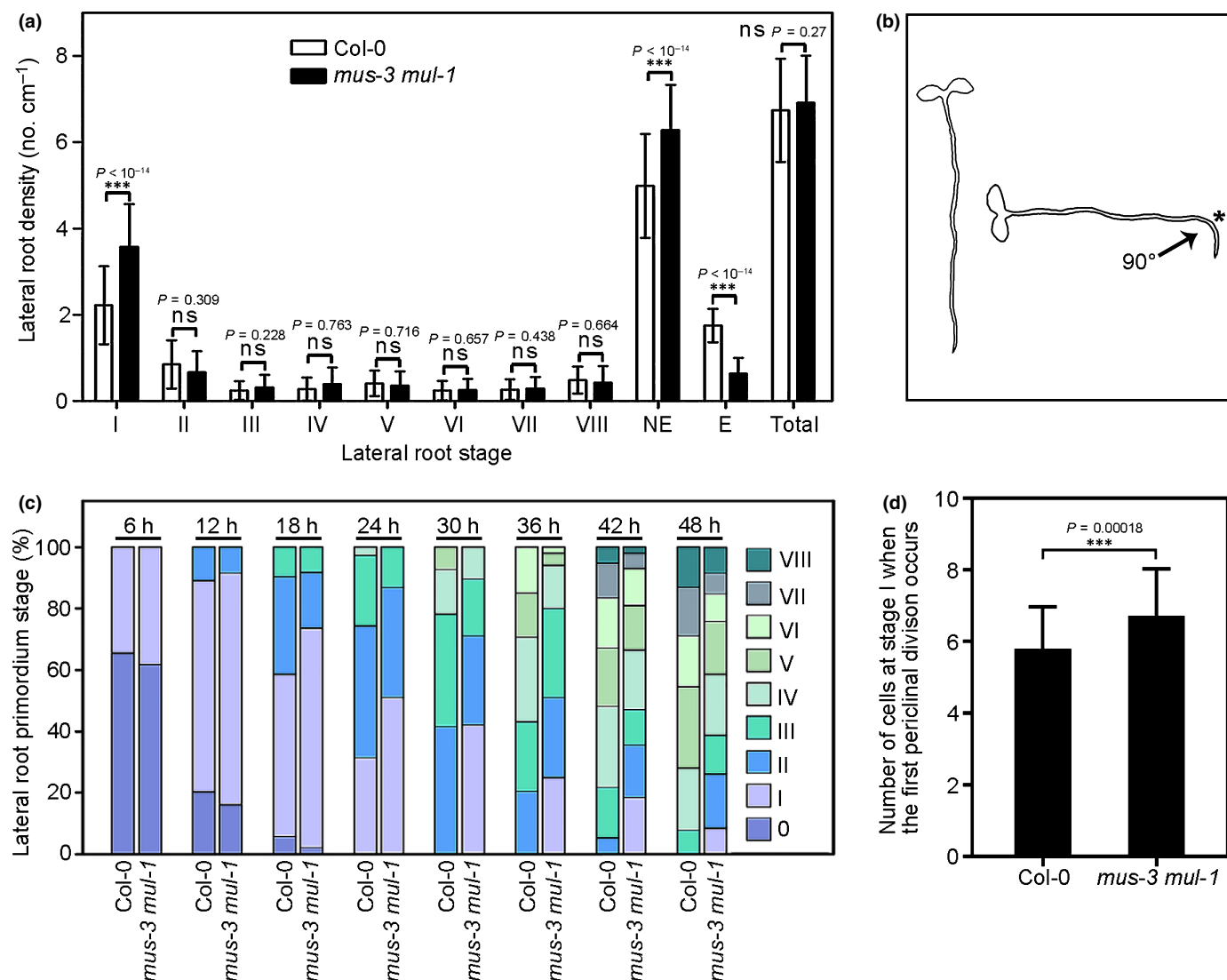
Fig. 4 Lateral root primordium development at stage I of *mus-3 mul-1* is significantly delayed. (a) Comparison of lateral root density of Col-0 and *mus-3 mul-1* at various developmental stages. Nine-day-old seedlings were used for analysis. Data shown represent average and SD ($n > 40$). Student's *t*-tests were used to compare the measurements of *mus-3 mul-1* with those from Col-0 (***, $P < 0.001$; ns, no significance at $P > 0.05$). (b) Diagram showing a classic approach which was used to induce lateral root initiation and formation. Bending the horizontally placed primary root tip 90° and allowing the root tip to grow in the direction of gravity can induce the initiation and formation of lateral roots at the convex side of the bending site, as indicated by an asterisk. (c) Measurements of the percentage of lateral root formation of Col-0 and *mus-3 mul-1* at various developmental stages ($n > 50$). Measurements were carried out every 6 h after the artificial induction shown in (b). (d) Number of primordium cells at stage I when the first periclinal division occurs in Col-0 ($n = 59$) and *mus-3 mul-1* ($n = 50$). Transgenic plants carrying *pDR5::GUS* in either Col-0 or *mus-3 mul-1* were used for the analyses as GUS staining can reveal the presence of lateral root primordia. NE, no emerged; E, emerged; Total, all lateral roots including lateral root primordia and emerged lateral roots. At least three independent biological replicates were carried out and consistent results were obtained. Results from one representative experiment are shown.

2014; Ramakrishna *et al.*, 2019; Vilches Barro *et al.*, 2019). We measured the width of lateral root founder cells in Col-0 and *mus-3 mul-1* before or after the first asymmetric division, using transgenic plants carrying *pPIN3::PIN3-GFP* in Col-0 and in *mus-3 mul-1*. We found no significant cell width difference in Col-0 and *mus-3 mul-1* (Fig. S4). These results indicated that the more time needed to finish stage I in *mus-3 mul-1* is partially due to the fact that additional cell divisions are required in comparison with that of Col-0.

MUS shows a polar localization in primary and lateral root cells

To understand the biological functions of MUS and MUL in regulating lateral root development, it is critical to know the protein localization of the two RLKs. Because transgenic plants carrying *pMUS::MUS-YFP* and *pMUL::MUL-YFP* in *mus-3 mul-1* were able to complement the lateral root defects of *mus-3 mul-1*, the localization of MUS-YFP and MUL-YFP observed in the

transgenic plants should represent its true protein localization. MUS can be detected in primary root meristem zone and in all eight developmental stages of lateral root primordia (Fig. 5a–k). Interestingly, MUS shows strong polar localization at anticlinal sides of the primary roots, the lateral root founder cells, and stage I lateral root primordia (Fig. 5a–o). We measured the mean fluorescence intensity of the MUS-YFP signal at the anticlinal and periclinal sides of cells in primary roots and stage I lateral roots. The polarity index is then calculated by dividing the anticlinal side fluorescence intensity by periclinal side fluorescence intensity (Fig. 5p). The polarity index is about 2.7 in primary roots and 2.5 in lateral roots. Polar localization of MUS was confirmed in transgenic plants carrying 35S::MUS-GFP. We found that MUS-GFP was located at the root-tip side of the cells in the primary roots (Fig. S5). Meanwhile, we analyzed protein localization of MUL in transgenic plants carrying pMUL::MUL-YFP and found no obvious polar localization (Fig. 5q–a1). MUL-YFP signal could be strongly observed in endodermis and weakly in pericycle and vascular cells of the primary root tips (Fig. 5q–s). Relatively weak MUL-YFP signal could be detected in lateral root primordia (Fig. 5t–a1).

IAA treatment can induce the expression of *MUS* in primary and lateral roots

Auxin plays important roles in all stages of lateral root formation. Some auxin-related mutants show similar phenotypes with *mus-3 mul-1* in lateral root development, such as a double mutant of auxin response factors, *arf7-1 arf19-1* (Fig. S6) (Okushima *et al.*, 2007; Ito *et al.*, 2016). We proposed that *MUS* may be regulated by auxin in regulating lateral root development. In order to examine the relationship between *MUS* and auxin, we treated *pMUS::GUS* transgenic plants with 1 µM IAA for 12 h and analyzed the GUS intensity by GUS staining. The *MUS* promoter activity was significantly enhanced after IAA treatment (Fig. S7). Detailed analysis showed that *MUS* promoter activity was enhanced mainly in the vascular tissues of primary roots and at early stages of lateral root primordia (Fig. 6a–l). However, based on GUS staining results, IAA treatment showed no obvious effects on *MUL* promoter activity in primary and lateral roots (Fig. 6m–x). We next performed qRT-PCR analysis to further examine the expression levels of *MUS* and *MUL* in Col-0 roots treated with 1 µM IAA for 3 h. The results showed that the expression level of *MUS* was increased more than eight-fold, the expression level of *MUL* was actually also increased by about 60% (Fig. 6y,z). Previous studies indicated that high concentration of auxin could regulate expression levels of its downstream target genes via auxin-mediated signaling pathways (Weijers *et al.*, 2005; Ito *et al.*, 2016). For example, auxin could up-regulate two transcription factors, ARF7 and ARF19. ARF7 and ARF9 could directly regulate the expression of their target genes to affect the lateral root growth and development (Okushima *et al.*, 2007). We examined the expression levels of *MUS* and *MUL* in *arf7-1 arf19-1* double mutant with or without the IAA treatment. Interestingly, the up-regulation of *MUS* and *MUL* by IAA was significantly decreased in *arf7-1 arf19-1* compared to

that in wild-type (Fig. 6y,z). These data suggest that auxin enhances the expression levels of *MUS* and *MUL* largely dependent on the function of ARF7 and ARF19.

MUS and MUL are kinase-inactive RLKs

MUS and MUL are two receptor kinases in the LRR VII subfamily. MUS contains 1140 amino acid residues, while MUL contains 1136 amino acid residues. Both proteins contain 25 LRRs in their extracellular domains. Generally, receptor kinases possess kinase activities which can phosphorylate downstream components to transmit extracellular signals. However, some receptor kinases show no kinase activity and they transmit signals mainly via protein–protein interactions (Castells & Casacuberta, 2007). Previous studies predicted that MUS is likely a kinase-inactive RLK (Castells & Casacuberta, 2007; Keerthisinghe *et al.*, 2015). To test the kinase activities of MUS and MUL, we carried out *in vitro* kinase assays. The cDNA sequences coding for the cytoplasmic domain of MUS and the kinase domain of CLV1 were cloned into a *pDEST15* vector. The resulting constructs encode MUS_{CD} and $CLV1_{KD}$ with an N-terminal in-frame fused GST tag, respectively. Whereas the cDNA sequence coding for the cytoplasmic domain of MUL was cloned into *pET-15b*. The resulting construct encodes MUL_{CD} with an N-terminal in-frame fused 6 X His tag. $GST-MUS_{CD}$, $His-MUL_{CD}$ and $GST-CLV1_{KD}$ were purified from *E. coli* and incubated in the kinase assay buffer supplemented with [γ-^{32}P]ATP. Kinase activity analysis via autoradiography showed that MUS and MUL did not exhibit any auto-phosphorylation or transphosphorylation (towards the substrate MBP, myelin basic protein) activity *in vitro*. CLV1, as a positive control, however, showed strong auto-phosphorylation and transphosphorylation activity towards MBP (Fig. 7a). In many kinase active RLKs, there is a conservative lysine (K) residue within their ATP binding motif. For example, K911 and K317 are these conservative lysine residues in the brassinosteroid receptor BRASSINOSTEROID INSENSITIVE1 (BRI1) and co-receptor BRI1-ASSOCIATED RECEPTOR KINASE (BAK1), respectively (Li *et al.*, 2002). In MUS and MUL, the corresponding residues are arginines (R), R867 for MUS and R869 for MUL. To test whether the natural occuring mutation from K to R resulted in the inactive kinases, we mutated R867 and R869 into K867 and K869, and glutamic acid (E) 867 and E869. We expected that MUS_{CD}^{R867K} and MUL_{CD}^{R869K} could regain kinase activities if the mutation from K to R is the reason for these two proteins to lose their kinase activities, whereas MUS_{CD}^{R867E} and, MUL_{CD}^{R869E} should not have kinase activities. We tested the kinase activities of these mutated proteins. Surprisingly, we found that all MUS_{CD}^{R867E}, MUS_{CD}^{R867K}, MUL_{CD}^{R869E}, MUL_{CD}^{R869K} still lacked kinase activities (Fig. 7a). These results showed that MUS and MUL are indeed kinase-inactive RLKs *in vitro*. At the meantime, we detected the phosphorylation levels of MUS, MUL and BARELY ANY MERISTEM 2 (BAM2) *in planta*. We constructed transgenic seedlings carrying *pUBQ10::MUS-FLAG*, *pUBQ10::MUL-FLAG*, and *pUBQ10::BAM2-FLAG* with the coding sequences of *MUS*, *MUL* and *BAM2* being cloned into *pBIB-BASTA-*
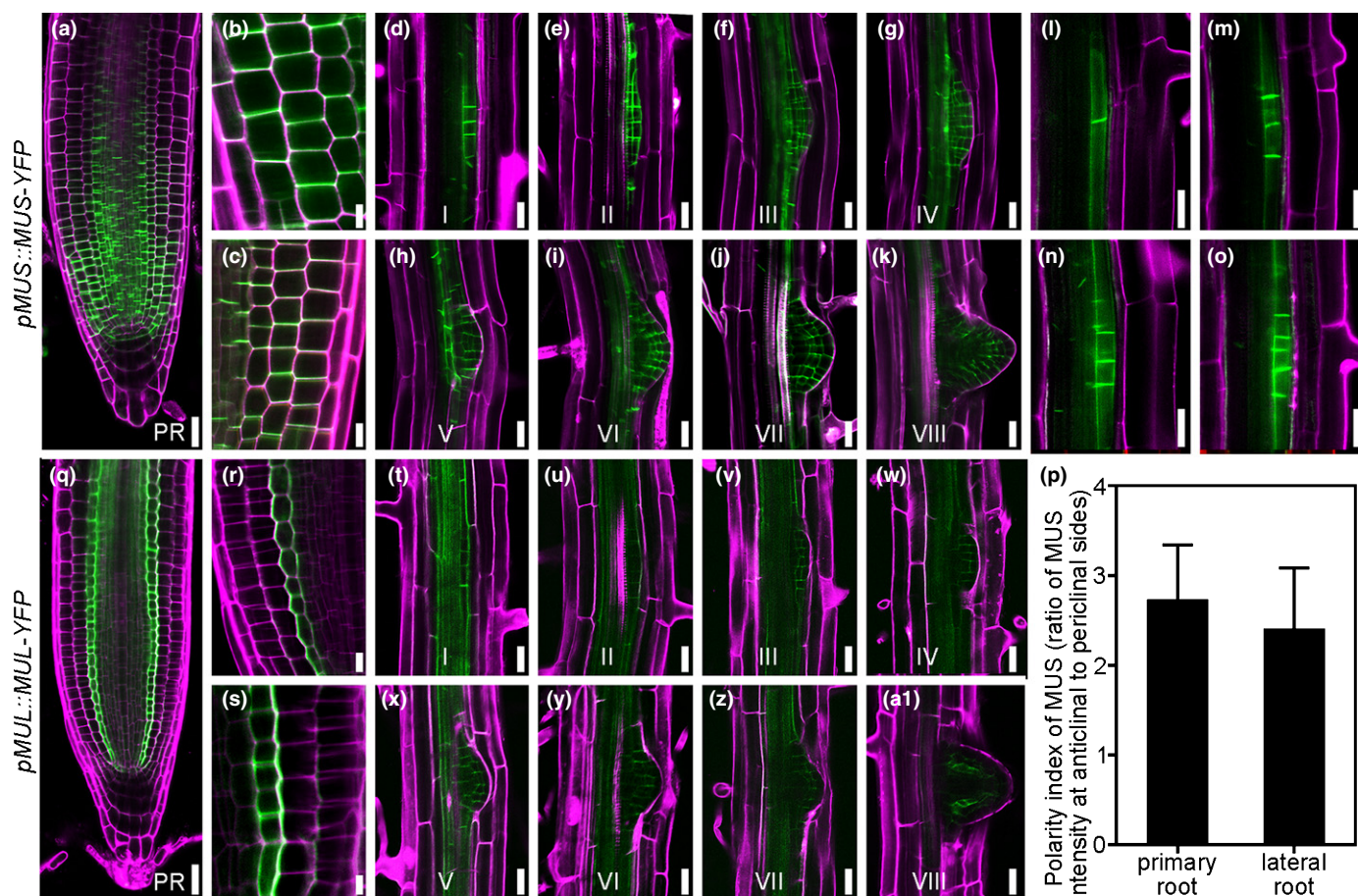
Fig. 5 MUS and MUL proteins can be detected in both primary and lateral roots, and MUS shows polar localization in primary and lateral root cells. (a–c) MUS-YFP from *pMUS::gMUS-YFP* transgenic plants can be visualized in the primary root meristematic zone and shows clear polar localization under a confocal microscope. (d–k) MUS-YFP can be detected at all eight developmental stages of lateral root primordia. (l–o) Different numbers of anticlinal cell divisions during early stages of lateral root development. MUS-YFP is mainly localized at the cell transverse side of lateral root founder cells and stage I lateral root primordia. (p) Polarity index of MUS-YFP in primary roots and stage I lateral root primordia (ratio of MUS intensity at anticlinal vs periclinal sides). Data shown represent average and SD ($n > 40$). (q–s) MUL-YFP from *pMUL::gMUL-YFP* transgenic plants can be detected in the endodermal cells of primary root without obvious polar localization under a confocal microscope. (t–a1) MUL-YFP shows weak signals during all eight developmental stages of lateral root primordia. Nine-day-old seedlings were stained with 100 ng μl^{-1} PI for 8 min before confocal analyses. Bars: (b, c, r, s) 5 μm; (a, d–o, q, t–a1) 25 μm. PR represents primary root. I–VIII represent the eight development stages of lateral root primordia.

UBQ10-GWR-FLAG. MUS-FLAG, MUL-FLAG and BAM2-FLAG were immunoprecipitated by anti-FLAG beads. The phosphorylation levels of these proteins were analyzed by using an anti-pThr antibody. Our results showed that all three fusion proteins were actually phosphorylated with the phosphorylation level of MUS much stronger than that of BAM2 *in planta*. MUL was also phosphorylated *in planta* and its phosphorylation level was slightly stronger than BAM2 but weaker than MUS (Fig. 7b).

MUS and MUL have no auto-phosphorylation activity *in vitro*, but are phosphorylated *in planta*, suggesting that there is another kinase *in planta* to phosphorylate MUS and MUL. We used MUS as an example to test whether the kinase activity of MUS is essential for its function, we detected the phosphorylation level of MUS^{R867E} *in planta* and found that it was similar to that of MUS (Fig. 7c). We next transformed *pMUS::MUS^{R867E}-GFP* into *mus-3 mul-1* and dozens of individual transgenic lines

were obtained. In most of these transgenic lines, *MUS^{R867E}* was able to complement the lateral root phenotypes of *mus-3 mul-1*. Two representative lines were analyzed in detail (Fig. 7d–g). These data suggest that MUS and MUL are kinase-inactive RLKs and affect the early development of lateral root primordia. Our result indicated that MUS functions independently of its kinase activity. In other words, the kinase activity of MUS is dispensable for its biological function.

The expression levels of cell wall related genes are significantly down-regulated in *mus-3 mul-1*

To investigate possible molecular mechanisms of MUS and MUL in regulating early lateral root development, we carried out an RNA-seq analysis to compare the transcription profiles of *mus-3 mul-1* with those of wild-type Col-0. Total RNA was extracted
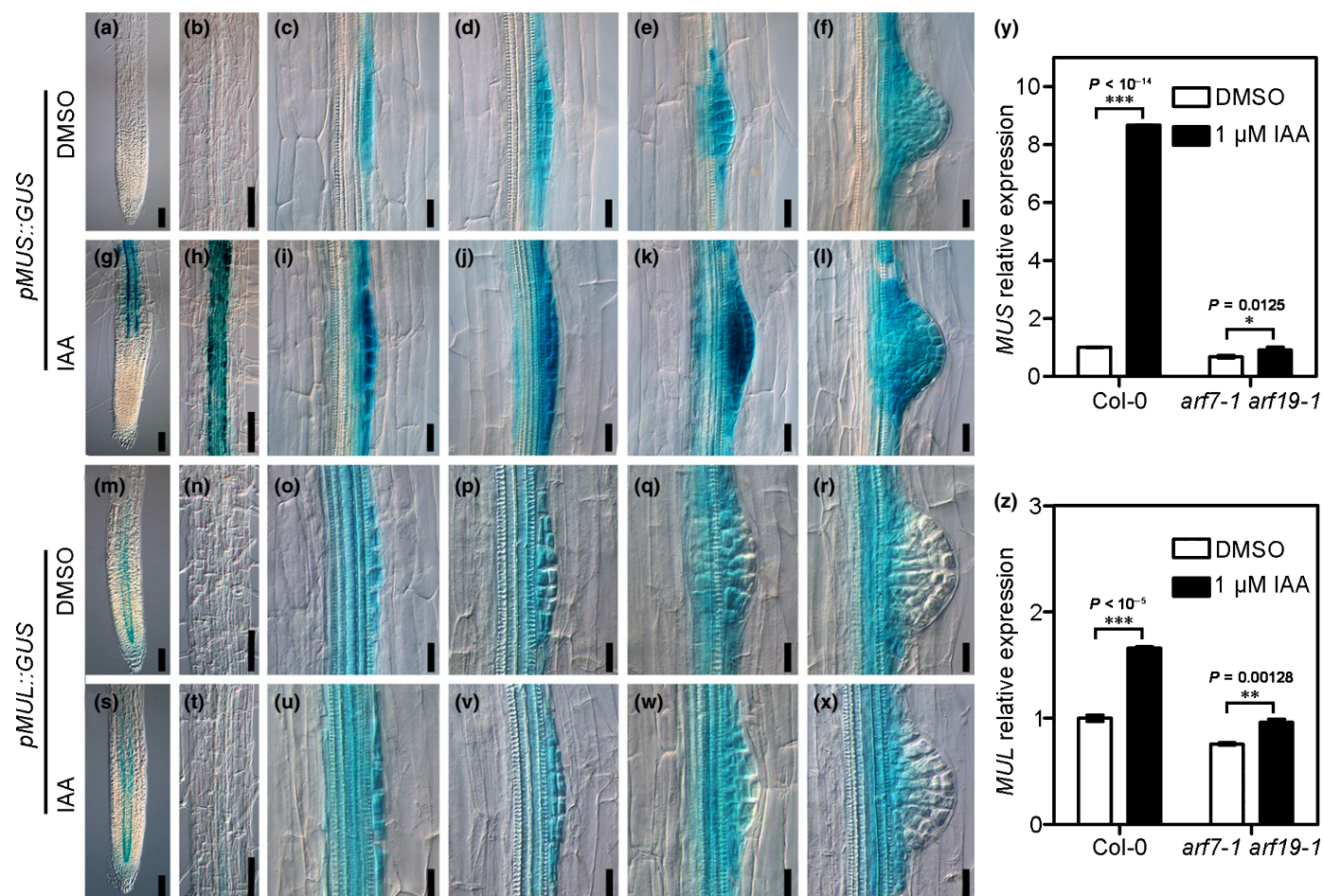
Fig. 6 IAA significantly upregulates the expression of *MUS* in an ARF7 and ARF19 dependent manner. (a–l) GUS stained roots from *pMUS::GUS* transgenic seedlings showing the expression of *MUS* is enhanced in the vasculature of root differentiation zone and at the early developmental stages of lateral root primordia. The *pMUS::GUS* transgenic roots were treated either with 0.01% DMSO as controls (a–f) or with 1 μM IAA (g–l) for 12 h. (m–x) GUS stained roots from *pMUL::GUS* transgenic seedlings indicating the upregulation of *MUL* after IAA treatment cannot be obviously observed in primary and lateral roots. *pMUL::GUS* transgenic seedlings treated with 0.01% DMSO were used as controls (m–r) or 1 μM IAA (s–x) for 12 h. Bars: (a, b, g, h, m, n, s, t) 100 μm; (c–f, i–l, o–r, u–x) 25 μm. (y, z) The relative expression levels of *MUS* and *MUL* in Col-0 and *arf7-1 arf19-1* without or with 1 μM IAA treatment for 3 h. Total RNA extracted from roots was used for qRT-PCR analyses. Data shown represent average and SD (*n* = 3). Student's *t*-test was used to compare the expression levels of *MUS* and *MUL* after treated with DMSO or IAA (***, *P* < 0.001; **, *P* < 0.01; *, *P* < 0.05). At least three independent biological replicates were performed and similar results were obtained. The data shown represent the results from one of the representative experiments.

from 7-d-old seedling roots of *mus-3 mul-1* and wild type Col-0. The obtained transcripts were analyzed by RNA-seq. Three biological replicates were performed. The volcano-plot distribution map showed relative expression of genes that differ more than two-fold between Col-0 and *mus-3 mul-1*. There were 136 differentially expressed genes based on a two-fold cutoff, including 39 up-regulated genes and 97 down-regulated genes in the double mutant relative to wild-type (Fig. 8a,b; Table S2). Thirteen of these down-regulated genes are classified as cell wall related and mapped by the expression clustering heatmap based on log2 (FPKM) (Fig. 8c). Nine of the 13 genes were further confirmed by qRT-PCR analysis (Fig. 8d). These nine genes include *At1G06520* (*GPAT1*), *At2G24980* (*EXTENSIN 6*), *At3G28300* (*AT14A*), *At3G62820*, *At4G33810*, *At4G37780* (*MYB87*), *At5G06640* (*EXTENSIN 10*), *At5G26080*, *At5G44400* (*ATBBE26*). We also analyzed the transcriptional levels of other cell wall remodeling genes which were found to be reduced at least 1.5-fold but less than two-fold based

on the RNA-seq results, such as *XYLOGLUCAN ENDOTRANSGLYCOSYLASE 6* (*XTR6*), *EXPANSIN 1* (*EXP1*), *EXP17* and *POLYGALACTURONASE ABSCISSION ZONE Arabidopsis thaliana* (*PGAZAT*). Our qRT-PCR results indicated that the transcriptional levels of these four genes were all down-regulated in *mus-3 mul-1* compared to wild-type (Fig. 8e) (Cai & Lashbrook, 2008; Ogawa *et al.*, 2009; González-Carranza *et al.*, 2012; Lee & Kim, 2013). Cell wall biosynthesis and remodeling are important during early development of lateral root primordia. For example, during the lateral root initiation, the lateral root founder cells expand and the stage I lateral root primordia show a distinct bulge. During these processes, the cell walls of overlying endodermal cells begin to relax, and endodermal cells undergo morphological changes, which promotes lateral root primordium emergence and lateral root development (Péret *et al.*, 2009; Vermeer *et al.*, 2014; Ramakrishna *et al.*, 2019). After multiple anticlinal divisions during stage I, new cell walls need to be synthesized.
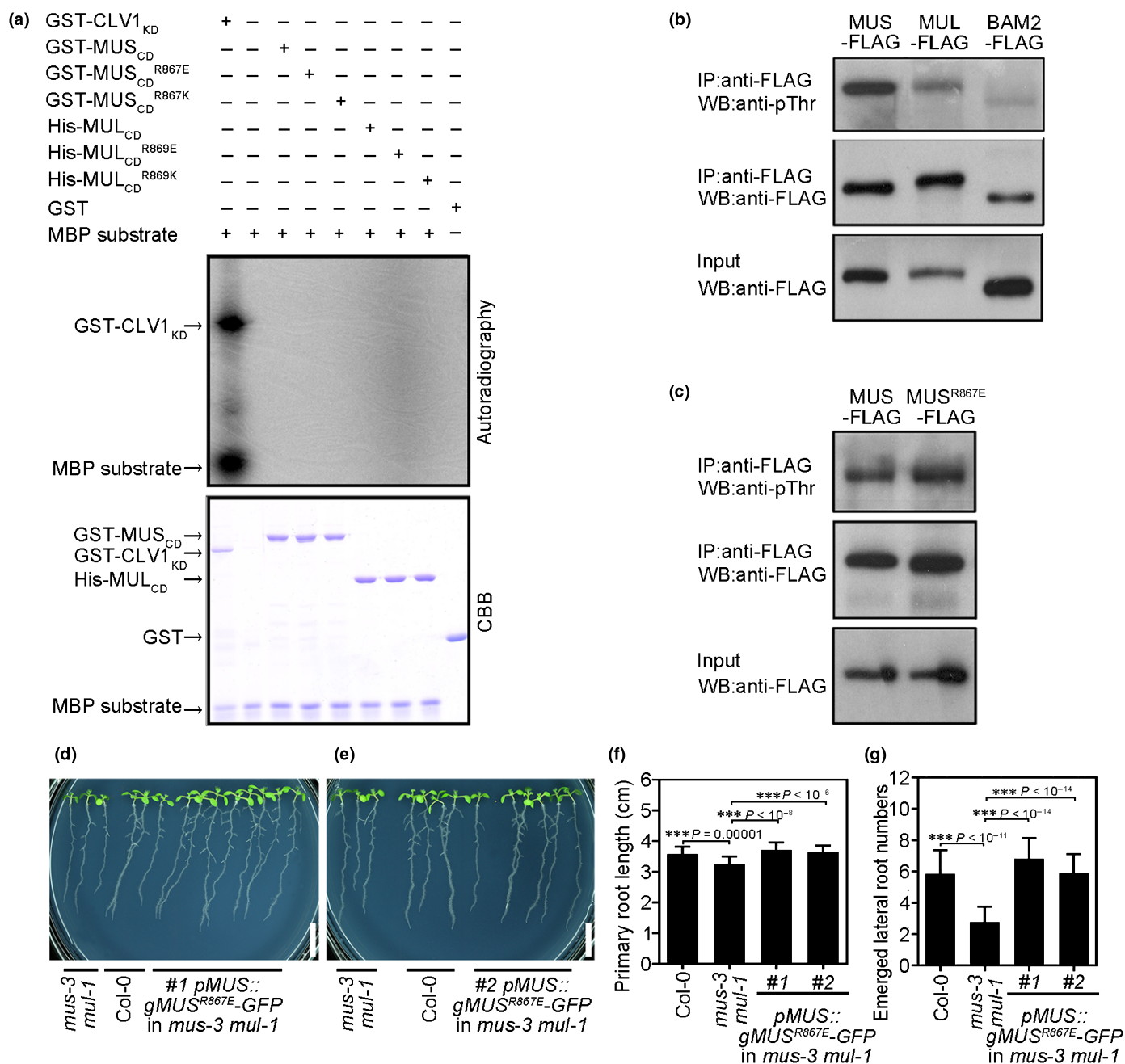
Fig. 7 MUS and MUL are kinase-inactive receptor-like kinases, and kinase activity is not essential for the function of MUS in regulating lateral root development. (a) The kinase activity assays indicate that MUS_{CD}, MUS_{CD}^{R867E}, MUS_{CD}^{R867K}, MUL_{CD}, MUL_{CD}^{R869E} and MUL_{CD}^{R869k} cannot be auto-phosphorylated *in vitro*. $CLV1_{KD}$ was used as a positive control. CBB, Coomassie brilliant blue. (b) The phosphorylation level of MUS is stronger than BAM2, a positive control, *in planta*. MUL can also be phosphorylated *in planta*. (c) MUS^R867E, in which an arginine residue in the ATP binding site was mutated to a glutamic acid, can still be phosphorylated *in planta*. *MUS-FLAG*, *MUL-FLAG*, *BAM2-FLAG* and *MUS^R867E-FLAG* were overexpressed and stable transgenic plants were obtained. (d, e) Mutation in the ATP binding site of MUS does not affect the biological function of MUS in lateral root development. Transgenic plants carrying *pMUS::MUS^R867E-GFP* can restore the developmental defects of the lateral roots of *mus-3 mul-1*. Seedlings were cultured on 1/5 MS medium for 8 d. Bars, 1 cm. (f, g) Measurements of primary root length and emerged lateral root numbers of Col-0, *mus-3 mul-1* and two independent transgenic lines #1, #2 of *pMUS::MUS^R867E-GFP* in *mus-3 mul-1*, respectively. Data shown represent average and SD (*n* > 35). Student's *t*-test was used to compare measurements from Col-0, two independent transgenic lines #1, #2 of *pMUS::MUS^R867E-GFP* in *mus-3 mul-1* with those from *mus-3 mul-1* (***, *P* < 0.001).

The RNA-seq results suggest that MUS and MUL regulate early lateral root primordium development possibly via mediating cell wall synthesis and remodeling (Fig. 9).

Discussion

Here, we report our identification of an *LRR-RLK* whose expression pattern appears to be very unique. This *LRR-RLK*
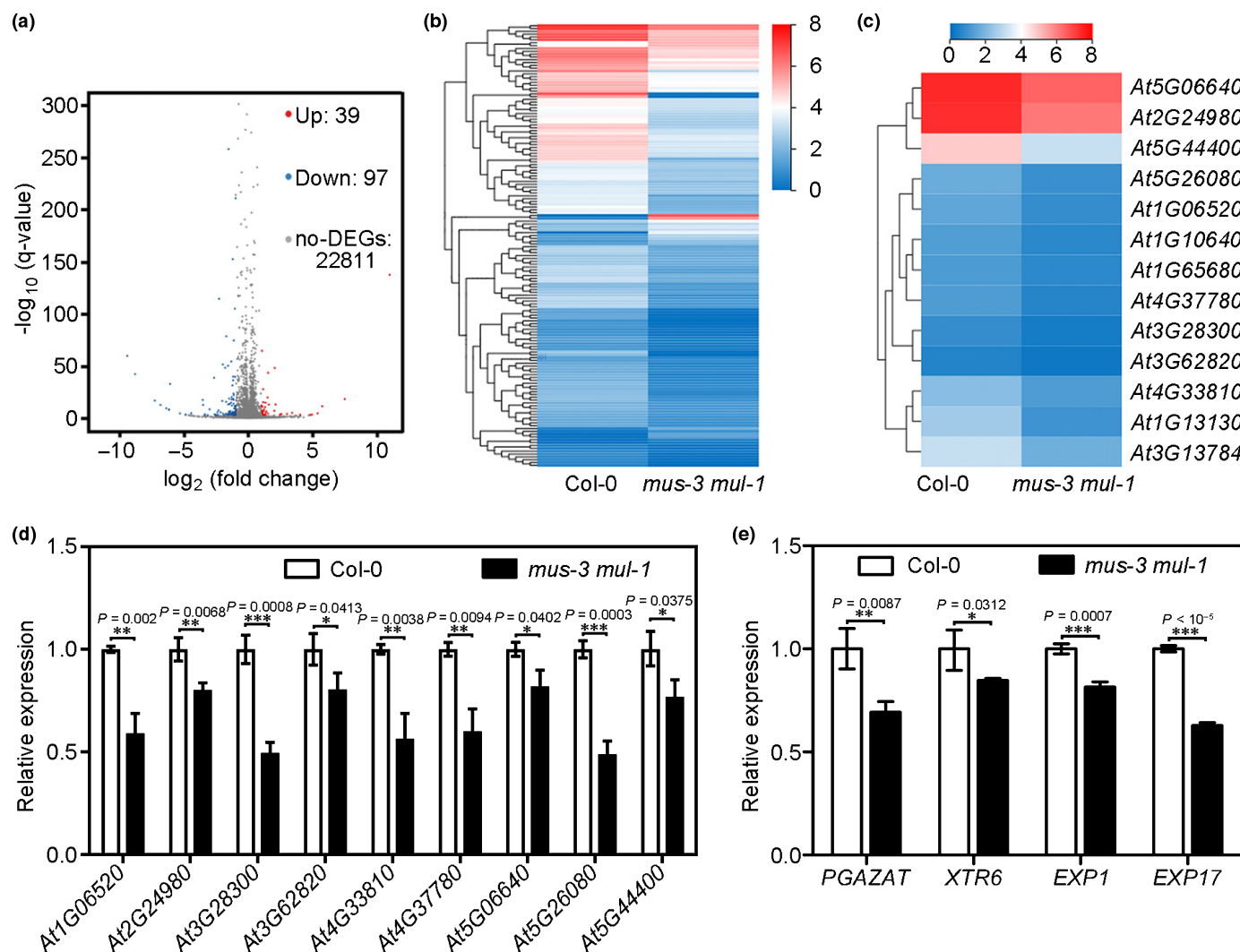
Fig. 8 A number of genes involved in cell wall biosynthesis and remodeling are significantly down-regulated in *mus-3 mul-1*. (a) The volcano-plot distribution map between Col-0 and *mus-3 mul-1*. Red dots represent up-regulated genes and blue dots represent down-regulated genes, fold change > 2 or < −2, *q*-value < 0.001. (b) The expression clustering heatmap of differentially expressed genes between Col-0 and *mus-3 mul-1*. Red and blue represent the expression after the conversion log2 (FPKM). (c) The expression clustering heatmap of cell wall-related genes between Col-0 and *mus-3 mul-1*. These genes were selected from the data shown in (b). (d) The transcriptional levels of cell wall-related genes are down-regulated in *mus-3 mul-1* compared to Col-0. (e) The transcriptional levels of several cell wall remodeling genes that have been reported in the literature are decreased in *mus-3 mul-1*. Total RNA extracted from 7-d-old seedling roots of Col-0 and *mus-3 mul-1* was used for qRT-PCR analyses. Three biological replicates for RNA sequencing were conducted for Col-0 and *mus-3 mul-1*. Data shown represent average and SD (*n* = 3). Student's *t*-test was carried out to test whether the data are significantly different between *mus-3 mul-1* and Col-0 (***, *P* < 0.001; **, *P* < 0.01; *, *P* < 0.05).

encodes a previously described protein named MUS. MUS protein was identified in stomata. The *mus* mutants show a stomatal bilateral asymmetry phenotype. Since our GUS staining data indicated that *MUS* is predominantly expressed in lateral root primordia and weakly expressed in primary roots (Fig. 1a–k), we proposed that MUS may also have a role in mediating lateral root development. To test this assumption, we isolated two independent T-DNA insertional lines for *MUS*, named *mus-3* and *mus-4*, and analyzed their possible defective phenotypes, especially in primary and lateral roots. Both alleles displayed a stomatal defect similar to what was reported previously (Keerthisinghe *et al.*, 2015), but they did not show any lateral root defects (Figs S3, S9, see later). We believed that failing to identify lateral root defects could be caused by functional

redundancy of MUS with its paralogs. Phylogenic analysis indicated that MUS is a member of LRR-RLK subfamily VII which consists of 10 total members (Fig. S1). We named its most closely related protein as MUSTACHES-LIKE (MUL). GUS staining analysis using transgenic plants carrying *pMUL::GUS* indicated that *MUL* promoter activity can be strongly detected in the vascular tissues of primary roots, stems, leaves, and areas where lateral root primordium initiates (Fig. 1l–v). Detailed protein localization analysis in transgenic plants carrying *pMUS::MUS-YFP* and *pMUL::MUL-YFP* further confirmed that these proteins are indeed localized in the lateral root primordia. The overlapped expression patterns in lateral root primordia further suggest that the two LRR-RLKs may redundantly regulate lateral root growth and development. Our
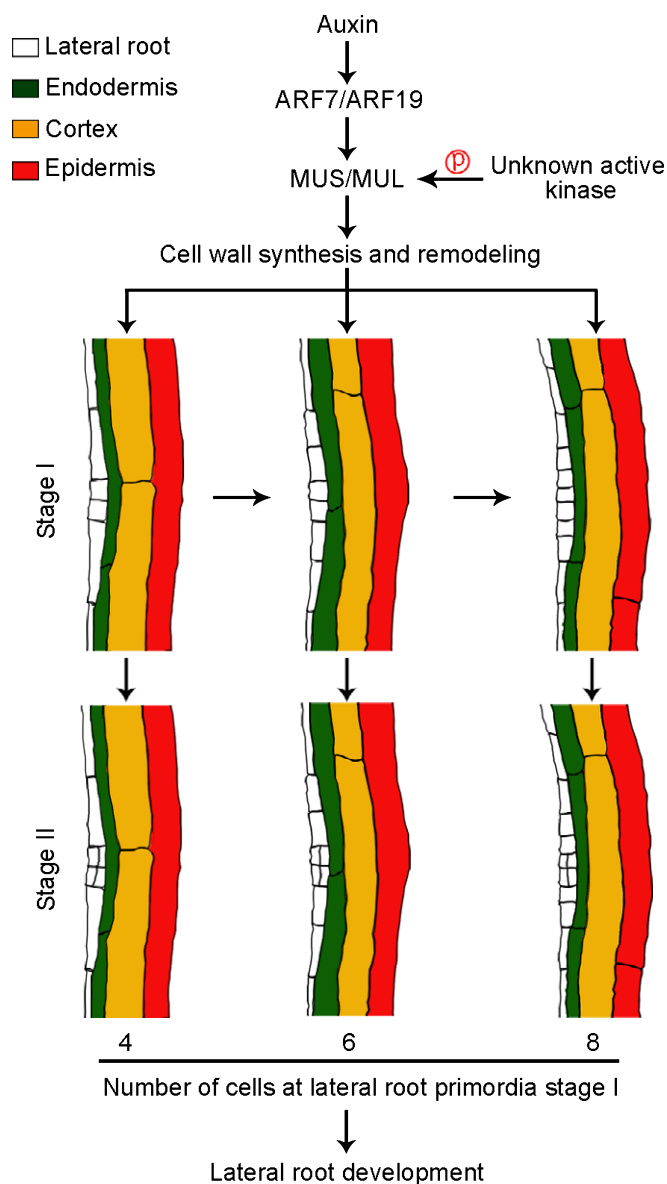
Fig. 9 A hypothetical model showing the roles of MUS and MUL in regulating lateral root development at stage I. Auxin can enhance the expression levels of *MUS* and *MUL* in primary and lateral roots. The regulation is largely dependent on ARF7 and ARF19. MUS and MUL, two kinase-inactive RLKs, can be phosphorylated by another unknown kinase *in planta* and control lateral root development at an early development stage through cell wall synthesis and remodeling. Diagram represents the early development of lateral root primordia in Col-0. Cell division is delayed due to impaired cell wall biosynthesis and remodeling at stage I of the lateral root development in *mus-3 mul-1*. In addition, more stage I cells are required for the double mutant before entering to stage II. These two defects lead to the retention of lateral root primordia at stage I in the double mutant.

detailed genetic and cell biology analyses suggested that MUS and MUL regulate lateral root development at stage I.

Our results showed that MUS and MUL are kinase-inactive receptor kinases, which can be phosphorylated by an unknown kinase *in planta* and transmit signals to regulate early lateral root development (Figs 7, 9). Our analyses confirmed that the kinase activity of MUS is dispensable for the function of MUS in lateral

root development. In *Arabidopsis thaliana*, sequence analysis found that nearly 20% of the RLKs are not conserved in their catalytic kinase domains, which were predicted to be kinase-inactive RLKs (Castells & Casacuberta, 2007). These kinase-inactive RLKs are also important in signal transduction and may act as scaffolds by interacting with other kinases (Kroiher *et al.*, 2001). For example, RECEPTOR DEAD KINASE1 (RDK1) is a kinase-dead RLK, and its kinase activity is not required for ABA-mediated early seedling development (Kumar *et al.*, 2017). The *Arabidopsis thaliana* CRINKLY4 RELATED 2 (AtCRR2) is a homolog of ACR4 and has no catalytic kinase activity. However, AtCRR2 could be phosphorylated by ACR4 *in vitro*, which indicates that AtCRR2 might act as heterodimer with the kinase-active ACR4 to regulate ACR4-mediated seed coat signaling (Cao *et al.*, 2005). STRUBBELIG (SUB) is also a kinase-inactive receptor kinase which plays an indispensable role in regulating root epidermal patterning (Chevalier *et al.*, 2005). To understand the detailed molecular mechanisms of MUS and MUL in regulating lateral root development will rely on the identification of an assumed kinase which can phosphorylate MUS and MUL *in planta*. Future genetic and proteomic approaches can be used to find such an active kinase.

Interestingly, MUS shows a polar localization in the primary and lateral root cells (Fig. 5a–o). This localization is similar to the polar distribution of an auxin efflux transporter PIN1, which has been reported to regulate lateral root development. *PIN1* expression can be detected in the vascular organization of primary roots, the lateral root founder cells and lateral root primordia cells (Omelyanchuk *et al.*, 2016). The polar localization of PIN1 determines the direction of auxin transport, leading to gradient distribution of auxin (Blilou *et al.*, 2005). Accumulation of auxin in lateral root founder cells can promote the formation of lateral root primordia (Benková *et al.*, 2003). Similar polar localization and similar biological function at lateral root development suggest that MUS and MUL may interact with PIN1. We therefore examined the protein level and localization of PIN1 in lateral root primordia of *mus-3 mul-1*. Our preliminary results indicated that the localization and protein level of PIN1 in lateral root primordia were not affected in *mus-3 mul-1* (Fig. S8). However, exogenous application of auxin could significantly enhance the expression of *MUS* in the early stages of lateral root development, which is dependent on the functions of ARF7 and ARF19 (Fig. 6). These data suggest that *MUS* and *MUL* are downstream components of auxin signaling pathway to regulate lateral root development. Whether MUS and MUL interact with PIN1 *in vivo* needs to be investigated in the future. It is worth noting that another member in the LRR VII subfamily, INFLORESCENCE AND ROOT APICES RECEPTOR KINASE (IRK), also shows polar distribution in the endodermis of Arabidopsis primary roots (Campos *et al.*, 2020). Whether additional members in this subfamily show polar localization is another interesting question to be explored.

RNA-seq data and qRT-PCR analyses showed the transcriptional levels of some cell wall synthesis and remodeling genes in *mus-3 mul-1* were down-regulated compared to Col-0 (Fig. 8). These data suggest that MUS and MUL control early lateral root

development likely via regulating cell wall synthesis and remodeling. It is possible that the cell division at stage I of *mus-3 mul-1* is delayed due to the cell wall biosynthesis defects. MUS localization analysis suggests that MUS is mainly accumulated at newly formed cell plates after the first few anticlinal cell divisions at stage I of lateral root primordium development (Fig. 5l–o). The observation that MUS is mainly accumulated at the newly formed cell plate during stage I is consistent with the RNA-seq results, both of which suggest that MUS and MUL may function in cell wall biosynthesis and remodeling at the early stages of lateral root development.

MUS and MUL may regulate microtubule arrangement. A previous report suggested that a loss-of-function mutant of *MUS* showed an altered stomatal bilateral symmetry phenotype due to defects in polarity growth and the radial arrangement of microtubules (Keerthisinghe *et al.*, 2015). We reinvestigated this result with our mutants. FM4-64 stained true leaves from 7-d-old seedlings were photographed using confocal fluorescence microscopy. Stomata of Col-0 and *mul* were bilaterally symmetrical, while stomata of *mus-3* and *mus-3 mul-1* display impaired bilateral symmetry (Fig. S9). These results are consistent with the observation from the previous report (Keerthisinghe *et al.*, 2015). In addition, the polar growth of microtubules affects cytoskeleton remodeling of pericycle and endodermis cells, which is required for the asymmetric expansion of founder cells when lateral root initiation occurs (Vilches Barro *et al.*, 2019). Thus, MUS and MUL may influence the early development of lateral root primordia at stage I partially through regulating the polar growth of microtubules. This issue also needs to be clarified in the future.

In summary, we proved MUS and MUL are two RLKs regulating early development of lateral root primordia. We propose that during lateral root primordium development, auxin can be accumulated in the center cells at stage I, which can upregulate the expression of *MUS* and *MUL*. As a result, cell division can be accelerated partially due to enhanced cell wall biosynthesis and remodeling. At the meantime, MUS and MUL also can promote the first periclinal cell division, allowing lateral root primordium to proceed into stage II (Fig. 9). Lateral roots are extremely critical for the entire architecture of the root system. Identification of RLKs in regulating lateral root initiation and development will help us to understand how environmental and developmental cures play significant roles in root system formation.

Data availability

Sequence data from this article can be found in The Arabidopsis Information Resource (http://www.arabidopsis.org/). Accession number: *MUS* (At1G75640), *MUL* (At4G36180), *ARF7* (At5G20730), *ARF19* (At1G19220), *CLV1* (At1G75820), *BAM2* (At3G49670), *PGAZAT* (At2G41850), *XTR6* (At4G25810), *EXP1* (At1G69530), *EXP17* (At4G01630).

Author contributions

JL, FET and QX designed all experiments, analyzed the data and wrote the manuscript. QX performed most of the experiments and prepared the data. YW and HL, contributed to generate the transgenic plants. YO, JC and KH participated in discussions and provided some suggestions for the project. XG provided GST-CLV1$_{KD}$ bacterial strain, and transgenic plant *pBIB-BASTA-UBQ10::BAM2-FLAG*.

ORCID

Xiaoping Gou (iD) https://orcid.org/0000-0002-8391-0258
Kai He (iD) https://orcid.org/0000-0003-0508-8411
Jia Li (iD) https://orcid.org/0000-0002-3148-6897
Frans E. Tax (iD) https://orcid.org/0000-0002-1386-3310
Qingqing Xun (iD) https://orcid.org/0000-0002-4049-4282

References

Araya T, Miyamoto M, Wibowo J, Suzuki A, Kojima S, Tsuchiya YN, Sawa S, Fukuda H, von Wiren N, Takahashi H. 2014. CLE-CLAVATA1 peptide-receptor signaling module regulates the expansion of plant root systems in a nitrogen-dependent manner. *Proceedings of the National Academy of Sciences, USA* **111**: 2029–2034.

Bellini C, Pacurar DI, Perrone I. 2014. Adventitious roots and lateral roots: similarities and differences. *Annual Review of Plant Biology* **65**: 639–666.

Benková E, Bielach A. 2010. Lateral root organogenesis – from cell to organ. *Current Opinion in Plant Biology* **13**: 677–683.

Benková E, Michniewicz M, Sauer M, Teichmann T, Seifertová D, Jürgens G, Friml J. 2003. Local, efflux-dependent auxin gradients as a common module for plant organ formation. *Cell* **115**: 591–602.

Bisseling T, Scheres B. 2014. Plant Science. Nutrient computation for root architecture. *Science* **346**: 300–301.

Blilou I, Xu J, Wildwater M, Willemsen V, Paponov I, Friml J, Heidstra R, Aida M, Palme K, Scheres B. 2005. The PIN auxin efflux facilitator network controls growth and patterning in *Arabidopsis* roots. *Nature* **433**: 39–44.

Cai SQ, Lashbrook CC. 2008. Stamen abscission zone transcriptome profiling reveals new candidates for abscission control: enhanced retention of floral organs in transgenic plants overexpressing Arabidopsis *ZINC FINGER PROTEIN2*. *Plant Physiology* **146**: 1305–1321.

Campos R, Goff J, Rodriguez-Furlan C, Van Norman JM. 2020. The Arabidopsis receptor kinase IRK is polarized and represses specific cell divisions in roots. *Developmental Cell* **52**: 183–195 e184.

Cao X, Li K, Suh SG, Guo T, Becraft PW. 2005. Molecular analysis of the *CRINKLY4* gene family in *Arabidopsis thaliana*. *Planta* **220**: 645–657.

Casimiro I, Beeckman T, Graham N, Bhalerao R, Zhang H, Casero P, Sandberg G, Bennett MJ. 2003. Dissecting *Arabidopsis* lateral root development. *Trends in Plant Science* **8**: 165–171.

Castells E, Casacuberta JM. 2007. Signalling through kinase-defective domains: the prevalence of atypical receptor-like kinases in plants. *Journal of Experimental Botany* **58**: 3503–3511.

Chevalier D, Batoux M, Fulton L, Pfister K, Yadav RK, Schellenberg M, Schneitz K. 2005. *STRUBBELIG* defines a receptor kinase-mediated signaling pathway regulating organ development in *Arabidopsis*. *Proceedings of the National Academy of Sciences, USA* **102**: 9074–9079.

Cho H, Ryu H, Rho S, Hill K, Smith S, Audenaert D, Park J, Han S, Beeckman T, Bennett MJ *et al.* **2014.** A secreted peptide acts on BIN2-mediated phosphorylation of ARFs to potentiate auxin response during lateral root development. *Nature Cell Biology* **16**: 66–76.

De Smet I, Vassileva V, De Rybel B, Levesque MP, Grunewald W, Van Damme D, Van Noorden G, Naudts M, Van Isterdael G, De Clercq R *et al.* **2008.** Receptor-like kinase ACR4 restricts formative cell divisions in the *Arabidopsis* root. *Science* **322**: 594–597.

Dimitrov I, Tax FE. **2018.** Lateral root growth in Arabidopsis is controlled by short and long distance signaling through the LRR RLKs XIP1/CEPR1 and CEPR2. *Plant Signaling & Behavior* **13**: e1489667.

Ditengou FA, Teale WD, Kochersperger P, Flittner KA, Kneuper I, van der Graaff E, Nziengui H, Pinosa F, Li X, Nitschke R *et al.* **2008.** Mechanical induction of lateral root initiation in *Arabidopsis thaliana. Proceedings of the National Academy of Sciences, USA* **105**: 18818–18823.

Dolan L, Janmaat K, Willemsen V, Linstead P, Poethig S, Roberts K, Scheres B. **1993.** Cellular organisation of the *Arabidopsis thaliana* root. *Development* **119**: 71–84.

Du Y, Scheres B. **2018.** Lateral root formation and the multiple roles of auxin. *Journal of Experimental Botany* **69**: 155–167.

Dubrovsky JG, Doerner PW, Colon-Carmona A, Rost TL. **2000.** Pericycle cell proliferation and lateral root initiation in Arabidopsis. *Plant Physiology* **124**: 1648–1657.

Gifford ML, Robertson FC, Soares DC, Ingram GC. **2005.** ARABIDOPSIS CRINKLY4 function, internalization, and turnover are dependent on the extracellular crinkly repeat domain. *Plant Cell* **17**: 1154–1166.

Gonneau M, Desprez T, Martin M, Doblas VG, Bacete L, Miart F, Sormani R, Hématy K, Renou J, Landrein B *et al.* **2018.** Receptor kinase THESEUS1 is a rapid alkalinization factor 34 receptor in *Arabidopsis. Current Biology* **28**: 2452–2458.

González-Carranza ZH, Shahid AA, Zhang L, Liu Y, Ninsuwan U, Roberts JA. **2012.** A novel approach to dissect the abscission process in Arabidopsis. *Plant Physiology* **160**: 1342–1356.

Gou X, He K, Yang H, Yuan T, Lin H, Clouse SD, Li J. **2010.** Genome-wide cloning and sequence analysis of leucine-rich repeat receptor-like protein kinase genes in *Arabidopsis thaliana. BMC Genomics* **11**: 19.

Ito J, Fukaki H, Onoda M, Li L, Li C, Tasaka M, Furutani M. **2016.** Auxin-dependent compositional change in Mediator in ARF7- and ARF19-mediated transcription. *Proceedings of the National Academy of Sciences, USA* **113**: 6562–6567.

Keerthisinghe S, Nadeau JA, Lucas JR, Nakagawa T, Sack FD. **2015.** The Arabidopsis leucine-rich repeat receptor-like kinase MUSTACHES enforces stomatal bilateral symmetry in Arabidopsis. *The Plant Journal* **81**: 684–694.

Kroiher M, Miller MA, Steele RE. **2001.** Deceiving appearances: signaling by "dead" and "fractured" receptor protein-tyrosine kinases. *BioEssays* **23**: 69–76.

Kumar D, Kumar R, Baek D, Hyun TK, Chung WS, Yun DJ, Kim JY. **2017.** *Arabidopsis thaliana RECEPTOR DEAD KINASE1* functions as a positive regulator in plant responses to ABA. *Molecular Plant* **10**: 223–243.

Kumpf RP, Shi CL, Larrieu A, Sto IM, Butenko MA, Péret B, Riiser ES, Bennett MJ, Aalen RB. **2013.** Floral organ abscission peptide IDA and its HAE/HSL2 receptors control cell separation during lateral root emergence. *Proceedings of the National Academy of Sciences, USA* **110**: 5235–5240.

Lee HW, Kim J. **2013.** *EXPANSINA17* up-regulated by LBD18/ASL20 promotes lateral root formation during the auxin response. *Plant and Cell Physiology* **54**: 1600–1611.

Li J, Tax FE. **2013.** Receptor-like kinases: key regulators of plant development and defense. *Journal of Integrative Plant Biology* **55**: 1184–1187.

Li J, Wen J, Lease KA, Doke JT, Tax FE, Walker JC. **2002.** BAK1, an Arabidopsis LRR receptor-like protein kinase, interacts with BRI1 and modulates brassinosteroid signaling. *Cell* **110**: 213–222.

Lynch J. **1995.** Root architecture and plant productivity. *Plant Physiology* **109**: 7–13.

Mähönen AP, Bishopp A, Higuchi M, Nieminen KM, Kinoshita K, Törmäkangas K, Ikeda Y, Oka A, Kakimoto T, Helariutta Y. **2006.** Cytokinin signaling and its inhibitor AHP6 regulate cell fate during vascular development. *Science* **311**: 94–98.

Malamy JE. **2005.** Intrinsic and environmental response pathways that regulate root system architecture. *Plant, Cell & Environment* **28**: 67–77.

Malamy JE, Benfey PN. **1997.** Organization and cell differentiation in lateral roots of *Arabidopsis thaliana. Development* **124**: 33–44.

Moreno-Risueno MA, Van Norman JM, Moreno A, Zhang J, Ahnert SE, Benfey PN. **2010.** Oscillating gene expression determines competence for periodic *Arabidopsis* root branching. *Science* **329**: 1306–1311.

Murphy E, Vu LD, Van den Broeck L, Lin Z, Ramakrishna P, van de Cotte B, Gaudinier A, Goh T, Slane D, Beeckman T *et al.* **2016.** RALFL34 regulates formative cell divisions in Arabidopsis pericycle during lateral root initiation. *Journal of Experimental Botany* **67**: 4863–4875.

Ogawa M, Kay P, Wilson S, Swain SM. **2009.** ARABIDOPSIS DEHISCENCE ZONE POLYGALACTURONASE1 (ADPG1), ADPG2, and QUARTET2 are polygalacturonases required for cell separation during reproductive development in *Arabidopsis. Plant Cell* **21**: 216–233.

Ohkubo Y, Tanaka M, Tabata R, Ogawa-Ohnishi M, Matsubayashi Y. **2017.** Shoot-to-root mobile polypeptides involved in systemic regulation of nitrogen acquisition. *Nature Plants* **3**: 17029.

Okushima Y, Fukaki H, Onoda M, Theologis A, Tasaka M. **2007.** ARF7 and ARF19 regulate lateral root formation via direct activation of *LBD/ASL* genes in *Arabidopsis. Plant Cell* **19**: 118–130.

Omelyanchuk NA, Kovrizhnykh VV, Oshchepkova EA, Pasternak T, Palme K, Mironova VV. **2016.** A detailed expression map of the PIN1 auxin transporter in *Arabidopsis thaliana* root. *BMC Plant Biology* **1**: 5.

Ou Y, Lu X, Zi Q, Xun Q, Zhang J, Wu Y, Shi H, Wei Z, Zhao B, Zhang X *et al.* **2016.** RGF1 INSENSITIVE 1 to 5, a group of LRR receptor-like kinases, are essential for the perception of root meristem growth factor 1 in *Arabidopsis thaliana. Cell Research* **26**: 686–698.

Parizot B, Laplaze L, Ricaud L, Boucheron-Dubuisson E, Bayle V, Bonke M, De Smet I, Poethig SR, Helariutta Y, Haseloff J *et al.* **2008.** Diarch symmetry of the vascular bundle in Arabidopsis root encompasses the pericycle and is reflected in distich lateral root initiation. *Plant Physiology* **146**: 140–148.

Péret B, Larrieu A, Bennett MJ. **2009.** Lateral root emergence: a difficult birth. *Journal of Experimental Botany* **60**: 3637–3643.

Ramakrishna P, Ruiz Duarte P, Rance GA, Schubert M, Vordermaier V, Vu LD, Murphy E, Vilches Barro A, Swarup K, Moirangthem K *et al.* **2019.** EXPANSIN A1-mediated radial swelling of pericycle cells positions anticlinal cell divisions during lateral root initiation. *Proceedings of the National Academy of Sciences, USA* **116**: 8597–8602.

Shiu SH, Bleecker AB. **2001.** Receptor-like kinases from *Arabidopsis* form a monophyletic gene family related to animal receptor kinases. *Proceedings of the National Academy of Sciences, USA* **98**: 10763–10768.

Tabata R, Sumida K, Yoshii T, Ohyama K, Shinohara H, Matsubayashi Y. **2014.** Perception of root-derived peptides by shoot LRR-RKs mediates systemic N-demand signaling. *Science* **346**: 343–346.

Toyokura K, Goh T, Shinohara H, Shinoda A, Kondo Y, Okamoto Y, Uehara T, Fujimoto K, Okushima Y, Ikeyama Y *et al.* **2019.** Lateral inhibition by a peptide hormone-receptor cascade during *Arabidopsis* lateral root founder cell formation. *Developmental Cell* **48**: 64–75 e65.

Van Norman JM, Xuan W, Beeckman T, Benfey PN. **2013.** To branch or not to branch: the role of pre-patterning in lateral root formation. *Development* **140**: 4301–4310.

Verbelen JP, De Cnodder T, Le J, Vissenberg K, Baluska F. **2006.** The root apex of *Arabidopsis thaliana* consists of four distinct zones of growth activities: meristematic zone, transition zone, fast elongation zone and growth terminating zone. *Plant Signaling & Behavior* **1**: 296–304.

Vermeer JE, von Wangenheim D, Barberon M, Lee Y, Stelzer EH, Maizel A, Geldner N. **2014.** A spatial accommodation by neighboring cells is required for organ initiation in *Arabidopsis. Science* **343**: 178–183.

Vilches Barro A, Stockle D, Thellmann M, Ruiz-Duarte P, Bald L, Louveaux M, von Born P, Denninger P, Goh T, Fukaki H *et al.* **2019.** Cytoskeleton dynamics are necessary for early events of lateral root initiation in *Arabidopsis. Current Biology* **29**: 2443–2454.

Vilches-Barro A, Maizel A. **2015.** Talking through walls: mechanisms of lateral root emergence in *Arabidopsis thaliana. Current Opinion in Plant Biology* **23**: 31–38.

Walker JC, Zhang R. 1990. Relationship of a putative receptor protein kinase
from maize to the S-locus glycoproteins of *Brassica*. *Nature* **345**: 743–746.

Weijers D, Benková E, Jager KE, Schlereth A, Hamann T, Kientz M, Wilmoth
JC, Reed JW, Jurgens G. 2005. Developmental specificity of auxin response by
pairs of ARF and Aux/IAA transcriptional regulators. *EMBO Journal* **24**: 1874–
1885.

Wu Y, Xun Q, Guo Y, Zhang J, Cheng K, Shi T, He K, Hou S, Gou X, Li J.
2016. Genome-wide expression pattern analyses of the *Arabidopsis* Leucine-rich
repeat receptor-like kinases. *Molecular Plant* **9**: 289–300.

Supporting Information

Additional Supporting Information may be found online in the
Supporting Information section at the end of the article.

Fig. S1 Phylogenetic analysis of LRR-RLKs from subfamily VII.

Fig. S2 The expression of *MUS* cannot be detected in the aerial
parts of Arabidopsis seedlings, while the expression of *MUL* can
be detected in the vasculature of the aerial parts.

Fig. S3 Single mutant *mus-3* or *mul-1* shows the root and above-
ground phenotypes similar to Col-0.

Fig. S4 The width of lateral root founder cells in Col-0 and *mus-
3 mul-1* showed no significant difference before or after the first
asymmetric division.

Fig. S5 MUS shows a polar localization in primary roots.

Fig. S6 The *arf7-1 arf19-1* double mutant shows a defective lat-
eral root phenotype.

Fig. S7 Auxin can upregulate the expression level of *MUS* in
roots.

Fig. S8 Protein levels and localization of an auxin efflux trans-
porter PIN1 are similar in Col-0 and *mus-3 mul-1*.

Fig. S9 MUS regulates stomatal bilateral symmetry and morpho-
genesis.

Table S1 Primers used in this study.

Table S2 Differentially expressed genes with fold change ≥ 2,
$P < 0.001$ in roots of Col-0 and *mus-3 mul-1*.

Please note: Wiley Blackwell are not responsible for the content
or functionality of any Supporting Information supplied by the
authors. Any queries (other than missing material) should be
directed to the *New Phytologist* Central Office.